March 2019

Variations of Sedimentary Biogenic silica in the Gulf of Mexico during the Deepwater Horizon and IXTOC-I Oil Spill.

Jong Jin Lee
University of South Florida, jongjinlee.001@gmail.com

Variations of Sedimentary Biogenic silica in the Gulf of Mexico during the

Deepwater Horizon and IXTOC-I Oil Spill.

by

Jong Jin Lee

A thesis submitted in partial fulfillment
of the requirements for the degree of
Master of Science
with a concentration in Geological Oceanography
College of Marine Science
University of South Florida

Major Professor: David J. Hollander, Ph.D.
Patrick T. Schwing, Ph.D
Brad E. Rosenheim, Ph.D
Isabel C. Romero, Ph.D

Date of Approval:
March 25, 2019

Keywords: Biogenic Silica, MOSSFA, Deepwater Horizon oil spill, IXTOC-I oil spill, Dam construction

Table of Contents

List of Tables

List of Figures

Abstract

The goal of this research is to understand the impacts of the 2010 Deepwater Horizon oil spill and the 1970-1980 IXTOC-I oil spill and other anthropogenic activity (e.g. dam construction) on surface water primary productivity by measuring sedimentary biogenic silica. It is known that sedimentary biogenic silica is distinct from mineral – bound silica, therefore it has been used as a proxy record for surface water primary productivity (e.g. diatom blooms). The Deepwater Horizon oil spill resulted in a widespread Marine Oil Snow Sedimentation and Flocculent Accumulation (MOSSFA) event. The IXTOC-I oil spill was one of the largest oil spills in history and it is likely that the MOSSFA event occurred as a direct result. MOSSFA is characterized by increased deposition of surface derived components and dramatic changes in post-depositional chemical (redox) and biological (benthic meio- and macro-fauna) conditions. Sedimentary biogenic silica provides an independent record of the surface derived portion of MOSSFA inputs. Occurrences of MOSSFA after IXTOC-I oil spill and Deepwater Horizon oil spill were compared by collecting sediment cores from the northern Gulf of Mexico (Deepwater Horizon) and the southern Gulf of Mexico (IXTOC-I). An age model for each core was developed using short-lived radioisotopes (i.e. $^{210}Pb_{xs}$). Sedimentary biogenic silica was significantly elevated in sedimentary intervals affected by the Deepwater Horizon spill. This suggests that a significant portion of the surface biological materials entrained during the MOSSFA event were sourced by diatom production. However, only one core (of three from the oil spill influenced area utilized in this study) from shallower depth had elevated levels of sedimentary biogenic silica in the sedimentary interval associated with IXTOC-I. Also, the

down-core profiles of sedimentary biogenic silica from the other cores collected in the southern Gulf of Mexico are consistent with the history of dam construction (1949 to 1989) on the Grijalva and Papaloapan river systems. These two river systems are the dominant freshwater and nutrient sources for primary production in the Bay of Campeche region in the southern Gulf of Mexico and therefore the dominant control on diatom productivity and sedimentary biogenic silica distribution. Consequently, distribution of annual fresh water outflow and nutrient supply has transitioned from seasonal (before 1940's) to stable (after 1980's). Overall, sedimentary biogenic silica provides an independent record of surface derived MOSSFA inputs and serves as a proxy for other anthropogenic influences related to surface primary productivity variability.

Chapter 1

1.1 Introduction

As oil exploration expands, especially in deep water, interests and concerns about oil spills have coincidently expanded. Deepwater and Ultra-deep water drilling in the northern Gulf of Mexico (NGOM) is expanding (Skogdalen et al., 2011). In this study, the NGOM and the southern Gulf of Mexico (SGOM) were chosen as research areas because each area has been subject to a large oil spill.

In the NGOM, the DWH oil spill occurred in April 20, 2010 (US Department of Interior, 2010). Over 210 million US gal of liquid oil over an 87-day span were discharged and 2.1 million US gal of dispersants (Corexit EC 9500A and EC9527A) were applied on the surface and at the wellhead at 1,500 m water depth (Atlas and Hazen, 2011; Kujawinski et al., 2011; MC Nutt et al., 2011; US Department of Interior, 2010). In the SGOM, the 1979-1980 IXTOC-I oil spill released 130 million US gal over a 10 months span to the Bay of Campeche and dispersant (Corexit 9527) was applied on the oil spilled area by air (Boehm and Flest, 1982; Farrington, 1980; Jernelöv and Lindén, 1981). The occurrence of the Marine Oil Snow Sedimentation Flocculent Accumulation (MOSSFA) event after the DWH oil spill was studied and found previously by using variation of biogeochemical proxies and optical analysis of satellite imagery and from the NGOM (e.g. Polycyclic Aromatic Hydrocarbon (PAH), sediment trap diatom frustules flux, diatom 16S RNA, chlorophyll anomalies, planktic foraminifera) (Brooks et al., 2015; Daly et al., 2016; Hu et al., 2011; Passow et al., 2012; Passow and Ziervogel, 2016;

Romero et al., 2015, 2017; Schwing et al., 2015, 2017, Yan et al., 2016). The MOSSFA is defined as phenomena of formation of Marine Oil Snow (MOS) and/or Oil Mineral and its settling and deposition to the seafloor (Daly et al., 2016; Passow et al., 2012; Passow and Ziervogel, 2016).

Chapter 2 and 3 constrain and compare the consequence of these two oil spill, the DWH oil spill and IXTOC-I oil spill, in combination with the surrounding environmental condition (e.g. river discharge, surface current change and formation) influencing primary productivity.

For this, sedimentary biogenic silica (Sedi-BSi) of sediment cores from the NGOM (DWH oil spill) and the SGOM (IXTOC-I oil spill) were measured by using a wet-alkaline extraction method modified from DeMaster (1981). Sedi-BSi has been used to track environmental changes, which affect marine surface water primary productivity such as long term and short term climate change) (Bidle et al., 2002; Nelson et al., 1995; Tréguer et al., 1995). Diatoms are known as the largest primary producer group in various marine environment including the Gulf of Mexico. Diatom constructs frustules by incorporating silica from the surround water (Hernández-Becerril et al., 2008; Licea et al., 2011; Qian et al., 2003; Strom and Strom, 1996). The frustules ultimately sink and are deposited to the seafloor. Thus, deposited biogenic silica (BSi) reflects environmental changes. BSi in deep sea sediment has been reported to be well preserved (up to ~ 86%) (DeMaster et al., 1996; Nelson et al., 1995; Tréguer et al., 1995). Measuring Sedi-BSi is relatively easy in comparison to other diatom indicators such as biomarker or genetic analyses (DeMaster et al., 1996; Nelson et al., 1995; Tréguer et al., 1995).

1.2 Goal of Research

Chapter 2

Chapter 2 is entitled "Elevated Rates of Sedimentary Biogenic Silica Deposition in the Northern Gulf of Mexico during the Deepwater Horizon Oil Spill" and focuses on variation of the Sedi-BSi caused by the DWH oil spill and the ensuing the MOSSFA event. Specifically, MOSSFA is identified as a potential cause for increased Sedi-BSi during DWH spill. The preservation of MOSSFA Sedi-BSi in the NGOM was also assessed.

Profiles of Sedi-BSi from the NGOM indicate increased values in the DWH influenced sedimentary interval. Several other surface derived MOSSFA proxies (PAH, diatom frustules, diatom 16S RNA, chlorophyll anomalies, planktic foraminifera) increased in the sedimentary interval corresponding to the DWH oil spill (Brooks et al., 2015; Daly et al., 2016; Hu et al., 2011; Romero et al., 2015, 2017; Schwing et al., 2015, 2017, Yan et al., 2016) and were coincident with increases in Sedi-BSi. Also, observation of increased Sedi-BSi in the cores from the same coring sites collected 4 to 6 years after the DWH oil spill implies preservation potential of Sedi-BSi (short term and long term time scales) in the NGOM.

Chapter 3

Chapter 3 is entitled "Variation of Sedimentary Biogenic Silica Deposition in the Southern Gulf of Mexico related to the IXTOC-I Oil Spill (1979 -80) and other influences." In chapter 3, the influence of the IXTOC-I oil spill on Sedi-BSi in the SGOM was assessed. Variations of the Sedi-BSi in the SGOM and the NGOM were compared in order to constrain the effect of oil spill on primary productivity and the occurrence of the MOSSFA event after IXTOC-I and DWH spills.

In the SGOM, Sedi-BSi was influenced by natural variation (e.g. variations of river discharge rates, upwelling by wind stress, seasonal current direction shifts, long and short term natural impacts) and anthropogenic (e.g. dam construction, oil spill) factors (Gómez, 2002; Martínez-López and Zavala-Hidalgo, 2009; Ruiz-Fernández et al., 2012; Salmeron-Garcia et al., 2011; Zavala-Hidalgo et al., 2003; Zavala-Hidalgo et al., 2006).

An increase in Sedi-BSi corresponding to the IXTOC-I spill was observed in only one sediment core among three cores from the Bay of Campeche in the SGOM. This is consistent with a MOSSFA event after the IXTOC-I oil spill. Surrounding environmental conditions of this coring site, which indicates increased Sedi-BSi after the IXTOC-I spill, were favorable for the MOSSFA event post IXTOC-I spill (e.g. high annual and seasonal primary productivity, nutrient availability, clay mineral input). Also, the environmental conditions were similar to the DWH oil spill in the NGOM. Vonk et al., 2015 suggested the probability of a MOSSFA event after the IXTOC-I spill was high according to their findings of spilled oil and high input of dispersant and clay mineral.

Dam constructions on the Grijalva and Papaloapan river systems affect annual and seasonal productivity of the research area. Variations in Sedi-BSi of sediment cores from the SGOM was consistent with dam constructions on the Grijalva and Papaloapan river systems. These river systems are the primary freshwater with nutrient source in the Bay of Campeche. Dam construction on these river systems stabilized river water discharge rates and the amount of nutrient input (Fabian Rivera-Trejo et al., 2010; Lázaro-Vázquez et al., 2018; Marengo, Athie & Calahorra, 2006; Papaloapan Ref). Thus, primary productivity in this research area was changed by dam construction.

The fundamental goal of this study is to answer two main questions: 1) What is the mechanism for variation of Sedi-BSi by massive oil spills and ensuing MOSSFA events? 2) Is the Sedi-BSi a proper indicator, and an independent, corroborative proxy for tracking MOSSFA events and oil spill influences on the environment?

1.3 References

Atlas, R.M. and Hazen, T.C., 2011. Oil biodegradation and bioremediation: a tale of the two worst spills in US history.

Bidle, K.D., Manganelli, M. and Azam, F., 2002. Regulation of oceanic silicon and carbon preservation by temperature control on bacteria. Science, 298(5600), pp.1980-1984.

Brooks, G.R., Larson, R.A., Schwing, P.T., Romero, I., Moore, C., Reichart, G.J., Jilbert, T., Chanton, J.P., Hastings, D.W., Overholt, W.A. and Marks, K.P., 2015. Sedimentation pulse in the NE Gulf of Mexico following the 2010 DWH blowout. PLoS One, 10(7), p.e0132341.

Boehm, P.D. and Fiest, D.L., 1982. Subsurface distributions of petroleum from an offshore well blowout. The Ixtoc I blowout, Bay of Campeche. Environmental Science & Technology, 16(2), pp.67-74.

Daly, K.L., Passow, U., Chanton, J. and Hollander, D., 2016. Assessing the impacts of oil-associated marine snow formation and sedimentation during and after the Deepwater Horizon oil spill. Anthropocene, 13, pp.18-33.

DeMaster, D.J., 1981. The supply and accumulation of silica in the marine environment. Geochimica et Cosmochimica acta, 45(10), pp.1715-1732.

DeMaster, D.J., Ragueneau, O. and Nittrouer, C.A., 1996. Preservation efficiencies and accumulation rates for biogenic silica and organic C, N, and P in high-latitude sediments: The Ross Sea. Journal of Geophysical Research: Oceans, 101(C8), pp.18501-18518.

Farrington, 1980. NOAA Ship RESEARCHER/Contract Vessel PIERCE Cruise to IXTOC-I Oil Spill: Overview and Integrative Data Assessment and Interpretation. National Oceanic and Atmospheric Administration

Gómez, R.A., 2002. Primary production in the southern Gulf of Mexico estimated from solar-stimulated natural fluorecence. Hidrobiológica, 12(1), pp.21-28.

Hernández-Becerril, D.U., García-Reséndiz, J.A., Monreal-Gomez, M.A., Signoret-Poillon, M. and Aldeco-Ramirez, J., 2008. Nanoplankton fraction in the phytoplankton structure in the southern Gulf of Mexico (April 2000). Ciencias Marinas, 34(1), pp.77-90.

Hu, C., Weisberg, R.H., Liu, Y., Zheng, L., Daly, K.L., English, D.C., Zhao, J. and Vargo, G.A., 2011. Did the northeastern Gulf of Mexico become greener after the Deepwater Horizon oil spill?. Geophysical Research Letters, 38(9).

Jernelöv, A. and Lindén, O., 1981. Ixtoc I: a case study of the world's largest oil spill. Ambio, pp.299-306.

Kujawinski, E.B., Kido Soule, M.C., Valentine, D.L., Boysen, A.K., Longnecker, K. and Redmond, M.C., 2011. Fate of dispersants associated with the Deepwater Horizon oil spill. Environmental science & technology, 45(4), pp.1298-1306.

Lázaro-Vázquez, A., Castillo, M.M., Jarquín-Sánchez, A., Carrillo, L. and Capps, K.A., 2018. Temporal changes in the hydrology and nutrient concentrations of a large tropical river: A nthropogenic influence in the L ower G rijalva R iver, M exico. River Research and Applications, 34(7), pp.649-660.

Licea, S., Zamudio, M.E., Moreno-Ruiz, J.L. and Luna, R., 2011. A suggested local regions in the Southern Gulf of Mexico using a diatom database (1979-2002) and oceanic hidrographic features. Journal of environmental biology, 32(4), p.443.

Marengo, H., Athie, L. and Calahorra, O., 2006. Extreme events in the Grijalva river hydroelectric system in the southeast of Mexico in 1999. Dams and Reservoirs, Societies and Environment in the 21st Century, pp.199-205.

Martínez-López, B. and Zavala-Hidalgo, J., 2009. Seasonal and interannual variability of cross-shelf transports of chlorophyll in the Gulf of Mexico. Journal of Marine Systems, 77(1-2), pp.1-20.

McNutt, M.K., Camilli, R., Guthrie, G.D., Hsieh, P.A., Labson, V.F., Lehr, W.J., Maclay, D., Ratzel, A.C. and Sogge, M.K., 2011. Assessment of flow rate estimates for the Deepwater Horizon/Macondo well oil spill. US Department of the Interior.

Nelson, D.M., Tréguer, P., Brzezinski, M.A., Leynaert, A. and Quéguiner, B., 1995. Production and dissolution of biogenic silica in the ocean: revised global estimates, comparison with regional data and relationship to biogenic sedimentation. Global Biogeochemical Cycles, 9(3), pp.359-372.

Passow, U., Ziervogel, K., Asper, V. and Diercks, A., 2012. Marine snow formation in the aftermath of the Deepwater Horizon oil spill in the Gulf of Mexico. Environmental Research Letters, 7(3), p.035301.

Passow, U. and Ziervogel, K., 2016. Marine snow sedimented oil released during the Deepwater Horizon spill. Oceanography, 29(3), pp.118-125.

Qian, Y., Jochens, A.E., Kennicutt Ii, M.C. and Biggs, D.C., 2003. Spatial and temporal variability of phytoplankton biomass and community structure over the continental margin of the northeast Gulf of Mexico based on pigment analysis. Continental Shelf Research, 23(1), pp.1-17.

Rivera-Trejo, F., Soto-Cortés, G. and Méndez-Antonio, B., 2010. The 2007 flood in Tabasco, Mexico: An integral analysis of a devastating phenomenon. International Journal of River Basin Management, 8(3-4), pp.255-267.

Romero, I.C., Schwing, P.T., Brooks, G.R., Larson, R.A., Hastings, D.W., Ellis, G., Goddard, E.A. and Hollander, D.J., 2015. Hydrocarbons in deep-sea sediments following the 2010 Deepwater Horizon blowout in the northeast Gulf of Mexico. PLoS One, 10(5), p.e0128371.

Ruiz-Fernandez, A.C., Sanchez-Cabeza, J.A., Alonso-Hernandez, C., Martínez-Herrera, V., Perez-Bernal, L.H., Preda, M., Hillaire-Marcel, C., Gastaud, J. and Quejido-Cabezas, A.J., 2012. Effects of land use change and sediment mobilization on coastal contamination (Coatzacoalcos River, Mexico). Continental Shelf Research, 37, pp.57-65.

Salmerón-García, O., Zavala-Hidalgo, J., Mateos-Jasso, A. and Romero-Centeno, R., 2011. Regionalization of the Gulf of Mexico from space-time chlorophyll-a concentration variability. Ocean Dynamics, 61(4), pp.439-448.

Schwing, P.T., Romero, I.C., Brooks, G.R., Hastings, D.W., Larson, R.A. and Hollander, D.J., 2015. A decline in benthic foraminifera following the Deepwater Horizon event in the northeastern Gulf of Mexico. PLoS One, 10(3), p.e0120565.

Schwing, P.T., Brooks, G.R., Larson, R.A., Holmes, C.W., O'Malley, B.J. and Hollander, D.J., 2017. Constraining the Spatial Extent of Marine Oil Snow Sedimentation and Flocculent Accumulation Following the Deepwater Horizon Event Using an Excess 210Pb Flux Approach. Environmental Science & Technology, 51(11), pp.5962-5968.

Skogdalen, J.E., Utne, I.B. and Vinnem, J.E., 2011. Developing safety indicators for preventing offshore oil and gas deepwater drilling blowouts. Safety science, 49(8-9), pp.1187-1199.

Strom, S.L. and Strom, M.W., 1996. Microplankton growth, grazing, and community structure in the northern Gulf of Mexico. Marine Ecology Progress Series, 130, pp.229-240.

Treguer, P., Nelson, D.M., Van Bennekom, A.J., DeMaster, D.J., Leynaert, A. and Quéguiner, B., 1995. The silica balance in the world ocean: a reestimate. Science, 268(5209), pp.375-379.

US Department of Interior. (2010, August 02). U.S. scientific teams refine estimates of oil flow from BP's well prior to capping. Retrieved December 16, 2010, from http://www.doi.gov/news/pressreleases/US-Scientific-Teams-Refine-Estimates-of-Oil-Flow-from-BP-Well-Prior-to-Capping.cfm.

Vonk, S.M., Hollander, D.J. and Murk, A.J., 2015. Was the extreme and wide-spread marine oil-snow sedimentation and flocculent accumulation (MOSSFA) event during the Deepwater Horizon blow-out unique?. Marine pollution bulletin, 100(1), pp.5-12.

Yan, B., Passow, U., Chanton, J.P., Nöthig, E.M., Asper, V., Sweet, J., Pitiranggon, M., Diercks, A. and Pak, D., 2016. Sustained deposition of contaminants from the Deepwater Horizon spill. Proceedings of the National Academy of Sciences, 113(24), pp.E3332-E3340.

Zavala-Hidalgo, J., Gallegos-García, A., Martínez-López, B., Morey, S.L. and O'Brien, J.J., 2006. Seasonal upwelling on the western and southern shelves of the Gulf of Mexico. Ocean dynamics, 56(3-4), pp.333-338.

Chapter 2

Elevated Rates of Sedimentary Biogenic Silica Deposition in the Northern Gulf of Mexico during the Deepwater Horizon Oil Spill.

Abstract

The 2010 Deepwater Horizon (DWH) oil spill resulted in a widespread Marine Oil Snow Sedimentation and Flocculent Accumulation (MOSSFA) event. MOSSFA is characterized by increased deposition of surface-derived components and dramatic changes in post-depositional chemical (redox) and biological (mass mortality of benthic meio- and macro-fauna) conditions. In an effort to constrain the effects of the DWH spill and MOSSFA, sedimentary biogenic silica (Sedi-BSi) were measured in sediment cores from the northern Gulf of Mexico (NGOM) utilizing a wet-alkaline extraction method modified from DeMaster (1981). As Sedi-BSi is distinct from mineral – bound silica, it has been used as a proxy record of diatom production and surface water primary productivity. Sedi-BSi significantly increased in the DWH-influenced sedimentary interval. This suggests that a significant portion of the surface biological materials entrained during the MOSSFA event were sourced by diatom production. Elevated Sedi-BSi coordinated well with previously measured proxies of diatom productivity (e.g. 16S-RNA, diatom frustules collected by sediment trap). Sedi-BSi results also corroborate existing records of other surface derived MOSSFA materials in 2010-2011 including planktonic foraminiferal tests, pyrogenic hydrocarbons, and other petroleum-derived biomarkers. Increases in Sedi-BSi in the

DWH-influenced sedimentary interval were well preserved in cores collected in 2016. Overall, Sedi-BSi provides an independent and corroborative proxy for surface-derived MOSSFA material deposited during the DWH.

2.1 Introduction

The Deepwater Horizon oil spill (DWH) occurred over an 87 day span (April 20 – July 15, 2010) (US Department of Interior, 2010). A total of over 210 million US gal of the liquid oil was released into the northern Gulf of Mexico (NGOM) (Atlas and Hazen, 2011; McNutt et al., 2011; US Department of Interior, 2010). Dispersants (about 2.1 million US gal of Corexit EC 9500A and EC9527A) were applied on the surface and at the wellhead (1,500 m water depth; Kujawinski et al., 2011). A Marine Oil Snow Sedimentation and Flocculent Accumulation (MOSSFA) event also occurred during and following the DWH oil spill (Daly et al., 2016).

The MOSSFA concept is described by the formation of Marine Oil Snow (MOS) and/or Oil-Mineral Aggregations (OMAs) and its settling and deposition to the seafloor (Daly et al., 2016). Natural marine snow is one of the most important mechanisms for the sinking of surface material to sea floor (Alldredge and Silver, 1988, Guidi et al., 2008). MOS is a combination of marine snow and byproducts of marine biota, oil, dispersant, and particles for the Mississippi River and continental shelf area (Daly et al., 2016; Passow et al., 2012; Passow and Ziervogel, 2016). MOSSFA enhanced the magnitude, changed the composition of the marine snow and altered biochemical processes in the NGOM after the DWH blowout (Daly et al., 2016; Passow et al., 2012; Passow and Ziervogel, 2016). An increase in phytoplankton populations produced more mucus and biopolymers, known as Exopolymeric Substance (EPS), and Transparent Exopolymeric Particles (TEP), in combination with the toxic stresses of oil and dispersant (Daly

et al., 2016; Gutierrez et al., 2013; Lincoln et al., Prep; Passow et al., 2012; Passow and Ziervogel, 2016). EPS and TEP are sticky materials secreted by surface water dwelling organisms (primary producers and consumers) that provide a matrix for the aggregation of particles for forming marine snow (Lincoln et al., Prep; Passow et al., 2012; Passow et al., 2016; Passow and Ziervogel, 2016). Clay-sized minerals are a major component of MOS and ballast heavier MOS particles (Daly et al., 2016; Passow et al., 2012; Passow and Ziervogel, 2016). The MOS settled on the ocean floor, transporting oil residues faster than it normally would (Daly et al., 2016; Romero et al., 2015; Schwing et al., 2017). The MOSSFA event impacted on the benthic ecology in association with oil contamination and low oxygen conditions (Baguley et al., 2015; Daly et al., 2016; Hastings et al., 2016; Montagna et al., 2013; Schwing et al., 2015; Wei et al., 2010).

The MOSSFA event was recorded by biogeochemical proxies from the NGOM (Schwing et al 2015; Brooks et al., 2015; Romero et al., 2015; Yan et al., 2016; Schwing et al. 2017; Romero et al., 2017). After the DWH blowout, phytoplankton blooms were observed in August 2010 in the NGOM (Hu et al., 2011; Murawski et al., 2016). This phytoplankton bloom was likely sustained by nutrients from the Mississippi River (Bianchi et al., 2011; O'Connor et al., 2016). The Mississippi and Atchafalaya river systems are primary sources of nutrients for primary production in the NGOM (Qian et al., 2003; Rabalais et al., 2007; Strom and Strom, 1996) and riverine influences induce diatom blooms, specifically (Daly et al., 2016; Lohrenz et al., 1997, 2008; Qian et al., 2003). The discharge from the Mississippi River controls the time, period, and intensity of the primary and diatom production in NGOM (Jochens et al., 2002; Lohrenz et al., 1997,2008). Diatoms are the largest primary producer group in this region and incorporate silica from the ambient water to construct frustules (Qian et al., 2003; Strom and

Strom, 1996). Sedimentary diatom production indicators include diatom frustules, diatom 16S RNA, and chlorophyll florescence anomalies, and sedimentary biogenic silica (Sedi-BSi). Previous research using these proxies identified diatom blooms during and following the DWH in sediment cores and water column (sediment traps) records (Brooks et al., 2015; Hu at al., 2011; Yan et al., 2016).

Sedi-BSi has been used as a proxy record of environmental events and surface water primary productivity in various marine environments (Nelson et al., 1995; Tréguer et al., 1995). Primary productivity is highly influenced by environmental change, whether it is natural or anthropogenic. The origin of Sedi-BSi is in the diatom's frustule. Biogenic silica (BSi) contents in sediment reflect diatom surface water productivity as diatoms incorporate silica from the ambient water to construct frustules and ultimately the frustules sink to the seafloor. Frustules are the largest part of diatom's body and mass, and are the most stable part of the organism. The variation of the surface water primary productivity and environmental changes can be estimated by measuring the Sedi-BSi (Bidle et al., 2002; Nelson et al., 1995; Tréguer et al., 1995). Sedi-BSi is relatively well preserved in deep sea sediment (up to ~86%) and easy to measure compared with other diatom indicators – biomarker or genetic (DeMaster et al., 1996; Nelson et al., 1995; Tréguer et al., 1995). Increasing Sedi-BSi was observed at the DWH influenced sedimentary interval and this is matched with other previously measured proxy records such as Polycyclic Aromatic hydrocarbons (PAH), diatom frustules, diatom 16S RNA, chlorophyll anomalies, planktic foraminifera (Brooks et al., 2015; Hu et al., 2011; Romero et al., 2015; Yan et al., 2016). Thus, Sedi-BSi is expected to be used as a corroborative proxy for massive oil spill and following MOSSFA event.

Sedi-BSi was measured in sediment cores collected in the NGOM and compared with other proxy records previously measured to answer two remaining questions: 1) How does Sedi-BSi vary after oil spills? 2) Is the Sedi-BSi a proper indicator, an independent, corroborative proxy for MOSSFA events in sediment records?

2.2 Methods

Field Sampling

Seven sediment cores were collected from four sites (DWH01, SW01, DSH08, and NT1200) using an MC-800 multicorer during the Center for Integrated Modeling and Analysis of Gulf Ecosystems (C-IMAGE) cruises from February 2011 to September 2016 (Fig. 1, Table 1). Site DWH01 is located near (<1km) the DWH wellhead (DSH08, 70 km; SW01, 87 km). NT1200 is located 250 km away from the blowout site and didn't show increasing hydrocarbon concentrations for both surface and subsurface plume related to DWH oil spill (Romero et al., 2015). Thus, site NT1200 is used as the control site. Cores were sub-sampled by extrusion at 2-5 mm intervals using a calibrated, threaded-rod extrusion device (Schwing et al., 2016) in order to conduct analysis for measuring various proxies including planktonic foraminiferal tests, biomarkers, grain size, and residues of the oil and dispersant. Extruded and sliced subsamples were freeze dried, ground, and homogenized to measure Sedi-BSi.

Sedi-BSi Analysis

Sedi-BSi was measured by using a wet-alkaline extraction method modified from DeMaster (1981) for this study. Freeze dried samples (10 ~ 20 mg) were put in a 50 ml conical centrifuge tube. Then 1N sodium hydroxide (30 ml) was added to each 50 ml conical centrifuge tube. These 50 ml conical centrifuge tubes were put in a water bath set to 85°C. The solution (0.1

ml) was extracted from each 50 ml conical centrifuge tubes 2, 3, 4, and 5 hours after the centrifuge tubes were put in the water bath. The extracted sample was injected to 15 ml conical centrifuge tubes with 2 ml of 0.1 hydrochloric acid.

Ammonium molybdate solution (6.5×10^{3}M) was added to each 15 ml centrifuge conical tubes at intervals of 15 minutes and reducing solution (solution of metol sulfite (0.15M), oxalic acid (1.1M), sulfuric acid (6.1N), and water) was added 15 minutes later. Absorbance of these final solutions in each 15 ml conical centrifuge tube was measured by using a spectrometer at the 812 nm wave length. Sedi-BSi are dissolved in the solution within 2 hours (DeMaster 1981). These are measured by extrapolating from measured increased silica concentration by mineral bound silica over time (2,3,4, and 5 hours).

Chronology

Each core was dated using short-lived radioisotope analysis to identify pre-, during, and post the DWH and IXTOC-I oil spill (Brooks et al, 2015; Schwing et al., 2017). Gamma spectrometry on Canberra HPGe (High-Purity Germanium) Coaxial Planar Photon Detectors was used to determine total ^{210}Pb, ^{214}Pb, and ^{214}Bi activities. The IAEA RGU-1 and IAEA-447 standards were used to correct for detector efficiency. The constant rate of supply (CRS) model was used to produce an age model for each core. The CRS model is appropriate for systems with varying accumulation rates of sediments (Appleby and Oldfield, 1983; Binford, 1990). Sedimentation rates were calculated based on these chronology and BSi-AR were achieved by multiplying Sedi-BSi contents (Sedi-BSi mass/ total sample mass) and sedimentation rates

Data Uncertainty

Three samples from the 2010 core at site DSH08 and two samples from the 2012 core at site SW01 were used to constrain data uncertainty of Sedi-BSi. Standard deviation of Sedi-BSi contents of selected samples ranged from 0.05% to 0.42%. Standard deviation of BSi-AR from selected samples indicate 0.45×10^{-4} g/cm^2/year to 2.70×10^{-4} g/cm^2/year. These standard deviations are 2.13% to 17.00% of the mean values. Each data uncertainty is marked with error bar at profiles (Fig 2A, 2C, Table 2C).

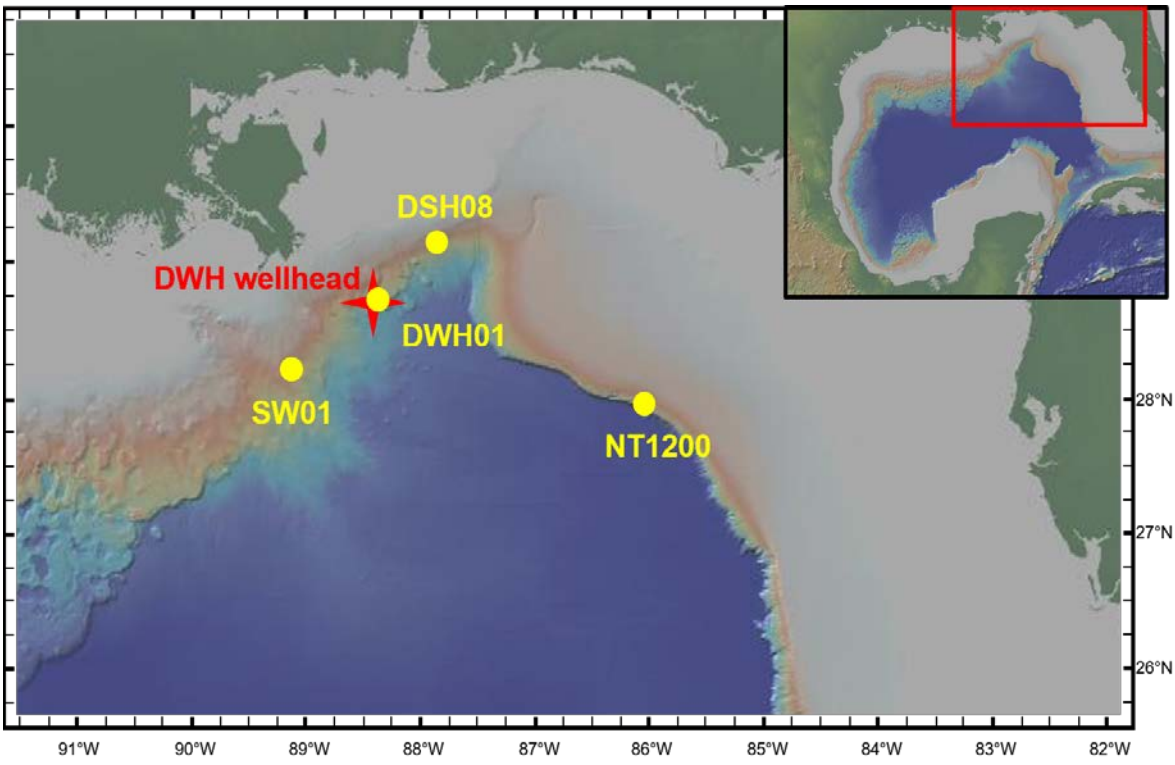

Fig 1. Coring sites in the NGOM and location of the DWH wellhead.

Table 1. Location and depth of coring sites in the NGOM and collection date.

NGOM	Latitude	Longitude	Water Depth (m)	Collection Date
DSH08-2011	29° 07.93 N	87° 52.00 W	1,100	02/20/2011
DWH01-2011	28° 44.74 N	88° 22.87 W	1,550	09/23/2011
SW01-2012	28° 14.34 N	89° 07.89 W	1,131	04/09/2012
NT1200-2011	27° 57.98 N	86° 01.39 W	1,200	06/27/2011
DSH08-2016	29° 07.25 N	87° 52.08 W	1,130	09/09/2016
DWH01-2016	28° 43.51 N	88° 23.24 W	1,577	09/08/2016
SW01-2016	28° 14.42 N	89° 07.30 W	1,132	09/08/2016

2.3 Results

Every core profile (except core from site NT1200; control site) was distinguished by 3 sub layers (Layer 1, Post-DWH; Layer 2, DWH; Layer 3, Pre-DWH) based on the variation of Sedi-BSi (Fig 2, Table 2). Layer 2 in each profile corresponded to 2010 ~ 2012 which represents the DWH influenced period. Layer 2 is defined as DWH spill influenced layer in this study. Layer 1 corresponds to post DWH spill (after 2011 ~ 2012) and layer 3 is before the DWH oil spill (before 2009~2010).

Layer 2 (DWH) of cores from site DSH08, DWH01, and SW01 shows increased values of Sedi-BSi. Layer 1 (Post-DWH) is the upper layer of DWH oil spill influenced Layer (layer 2) and its Sedi-BSi decreases. Layer 3 (Pre-DWH) is below (deposited prior to) layer 2 and has lower values than Layer 2 (Fig 2A ~ 2C, Table 2A). However, Sedi-BSi from site NT1200 did not vary considerably post-, during, and pre-DWH spill. The average of the NT1200 core is 1.1% and standard deviation is 0.25% (Fig 2D, Table 2B).

In the case of profiles of the 2011 core from site DSH08, the average of Sedi-BSi of Layer 1 (2010 ~ 2011), Layer 2 (2009), and Layer 3 (2001 ~ 2006) is 2.9%, 3.7%, and 4.0% respectively. The standard deviations (Stdev) are 0.4% (Layer 1), 1.3% (Layer 2), and 0.6% (Layer 3). The chronology for DSH08 in 2011 suggests that layer 2 is prior to the DWH oil spill.

However, the uncertainty of the chronology is 1.3 years in this interval and therefore Layer 2 could reflect the DWH spill. The average of BSi-AR of Layer 1, 2, and 3 is, 25.4×10^{-4} g/cm^2/year (Stdev: 4.1×10^{-4} g/cm^2/year), 47.0×10^{-4} g/cm^2/year (Stdev: 22.1×10^{-4} g/cm^2/year), and 35.1×10^{-4} g/cm^2/year (Stdev: 2.8×10^{-4} g/cm^2/year) respectively. The average Sedi-BSi of Layer 2 is 26.6% (Sedi-BSi contents) and 56.5% (BSi-AR) increased compared to Layer 3. Highest value of Layer 2 is 49.7% (Sedi-BSi contents) and 98.0% (BSi-AR) increased compared to lowest values of Layer 3 (Fig 2A, Table 2A).

The average Sedi-BSi contents is 2.4% (Layer 1; Stdev: 0.1%), 2.9% (Layer 2; Stdev: 0.8%), 2.4% (Layer 3; Stdev: 0.5%) in the 2016 core collected at DSH08. The average Sedi-BSi contents of Layer 2 is 50.9% increase compared to Layer 3. Highest value of Layer 2 is 140.8% (Sedi-BSi contents) increased compared to lowest values of Layer 3 (Fig 2A, Table 2A).

2011 core from site DWH01 indicates the average of 2.0% (Stdev: 0.6%), 2.6% (Stdev: 0.6%), and 1.7% (Stdev: 0.7%) of Sedi-BSi at Layer 1 (2011 ~2012), Layer 2 (2010 ~ 2011), and Layer 3 (2002 ~ 2009) respectively. The average BSi-AR of Layer 1, 2, and 3 is 23.9×10^{-4} g/cm^2/year (Stdev: 7.8×10^{-4} g/cm^2/year), 33.8×10^{-4} g/cm^2/year (Stdev: 7.3×10^{-4} g/cm^2/year), and 21.5×10^{-4}g/cm^2/year (Stdev: 9.4×10^{-4} g/cm^2/year) respectively. The average Sedi-BSi of Layer 2 is 53.9% (Sedi-BSi contents) and 57.0% (BSi-AR) increased compared to Layer 3. Highest value of Layer 2 is 278.0% (Sedi-BSi contents) and 322.4% (BSi-AR) increased compared to lowest values of Layer 3 (Fig 2B, Table 2A).

In the case of profiles of the 2016 core from site DWH01, the average of Sedi-BSi contents is 3.1% (Layer 1), 3.2% (Layer 2; Stdev: 1.0%), 2.0% (Layer 3; Stdev: 0.3%). The average Sedi-BSi of Layer 2 is 62.0% (Sedi-BSi contents) compared to Layer 3. Highest value of

Layer 2 is 315.8% (Sedi-BSi contents) increased compared to lowest values of Layer 3 (Fig 2B, Table 2A).

2012 core from site SW01 indicates the average of 1.4%, 2.3% (Stdev: 0.3%), and 1.7% (Stdev: 0.3%) of Sedi-BSi contents at Layer 1, 2, and 3 respectively. The average BSi-AR of Layer 1, 2, and 3 is 8.1×10^{-4} g/cm^2/year , 14.9×10^{-4} g/cm^2/year (Stdev: 1.6×10^{-4} g/cm^2/year), and 18.9×10^{-4} g/cm^2/year (Stdev: 6.6×10^{-4} g/cm^2/year) respectively. The average Sedi-BSi of Layer 2 is 39.5% (Sedi-BSi contents) and -21.2% (BSi-AR) increased compared to Layer 3. Highest value of Layer 2 is 89.3% (Sedi-BSi contents) and 52.45% (BSi-AR) increased compared to lowest values of Layer 3 (Fig 2C, Table 2A).

In the case of profiles of the 2016 core from site SW01, the average of Sedi-BSi contents is 1.9% (Layer 1; Stdev: 0.2%), 2.3% (Layer 2; Stdev: 0.4%), 1.9% (Layer 3; Stdev: 0.3%). The average Sedi-BSi of Layer 2 is 22.0% (Sedi-BSi contents) compared to Layer 3. Highest value of Layer 2 is 98.6% (Sedi-BSi contents) increased compared to lowest values of Layer 3 (Fig 2C, Table 2A).

Table 2. Sedi-BSi with depth (2010 to 2012 and 2016 cores) and chronology (2010 to 2012 cores) for each cores.

A

DSH08-2011	Depth (mm)	Sedi-BSi Contents (%)	BSi-AR ($g/cm^2/yr$)	Date (Year)			DSH08-2016	Depth (mm)	Sedi-BSi Contents (%)
				Average	Top of Interval	Bottom of Interval			
Layer 1	0	3.1	26.3×10^{-4}	2010.96	2011.14	2010.78	Layer 1	0	2.4
	2	3.2	29.1×10^{-4}	2010.52	2010.78	2010.25		2	2.6
	4	2.5	21.0×10^{-4}	2009.98	2010.25	2009.71		4	2.3
	Avg.	2.9	25.4×10^{-4}					6	2.5
Layer 2	6	2.3	21.7×10^{-4}	2009.43	2009.71	2009.15		8	2.2
	8	5.0	63.1×10^{-4}	2008.94	2009.15	2008.73		Avg.	2.4
	10	3.9	56.0×10^{-4}	2008.53	2008.73	2008.32	Layer 2	10	3.0
	Avg.	3.7	47.0×10^{-4}					12	4.0
Layer 3	20	3.3	36.6×10^{-4}	2005.87	2006.15	2005.59		14	2.0
	24	4.0	31.9×10^{-4}	2004.36	2004.81	2003.91		16	2.7
	32	4.6	36.8×10^{-4}	2001.02	2001.45	2000.59		Avg.	2.9
	Avg.	4.0	35.1×10^{-4}					18	1.7
								20	2.3
								25	2.4
								30	2.8
								Avg.	2.4
DWH01-2011	**Depth (mm)**	**Sedi-BSi Contents (%)**	**BSi-AR ($g/cm^2/yr$)**	**Date (Year)**			**DWH01-2016**	**Depth (mm)**	**Sedi-BSi Contents (%)**
				Average	**Top of Interval**	**Bottom of Interval**			
Layer 1	0	1.5	18.4×10^{-4}	2011.6	2011.8	2011.4	Layer 1	0	3.1
	2	2.4	29.4×10^{-4}	2011.3	2011.4	2011.1	Layer 2	2	3.4
	Avg.	2.0	23.9×10^{-4}					4	4.5
Layer 2	4	3.3	40.2×10^{-4}	2010.9	2011.1	2010.7		6	3.4
	6	2.1	25.9×10^{-4}	2010.4	2010.7	2010.2		8	3.2
	8	2.5	35.3×10^{-4}	2009.9	2010.2	2009.7		10	3.6
	Avg.	2.6	33.8×10^{-4}					12	3.4
Layer 3	10	2.4	30.5×10^{-4}	2009.4	2009.7	2009.1		14	1.1

Table 2. (Continued)

	20	2.1	27.2×10^{-4}	2005.7	2006.6	2004.9		Avg.	3.2
	25	1.5	18.9×10^{-4}	2004.0	2004.9	2003.0	Layer 3	16	1.7
	30	0.9	9.5×10^{-4}	2002.1	2003.0	2011.1		18	1.8
	Avg.	1.7	21.5×10^{-4}					20	1.9
								25	2.3
								30	2.4
								Avg.	2.0
SW01-2012	**Depth (mm)**	**Sedi-BSi Contents (%)**	**BSi-AR ($g/cm^2/yr$)**	**Date (Year)**			**SW01-2016**	**Depth (mm)**	**Sedi-BSi Contents (%)**
				Average	**Top of Interval**	**Bottom of Interval**			
Layer 1	0	1.4	8.1×10^{-4}	2012.2	2012.3	2011.8S	Layer 1	0	1.7
Layer 2	2	2.5	16.5×10^{-4}	2011.7	2011.8	2011.2		2	2.0
	4	2.5	14.0×10^{-4}	2010.9	2011.2	2010.3		Avg.	1.9
	6	1.9	13.0×10^{-4}	2009.9	2010.3	2009.3	Layer 2	4	2.8
	Avg.	2.3	14.5×10^{-4}					6	2.3
Layer 3	8	1.3	10.4×10^{-4}	2009.0	2009.3	2008.4		8	2.2
	20	1.6	21.0×10^{-4}	2004.6	2004.8	2004.2		10	1.9
	24	2.1	26.2×10^{-4}	2003.4	2003.6	2002.9		Avg.	2.3
	30	1.6	17.8×10^{-4}	2001.1	2001.3	2000.5	Layer 3	12	1.4
	Avg.	1.7	18.9×10^{-4}					14	1.8
								16	1.9
								18	1.9
								20	1.8
								25	2.1
								30	2.3
								Avg.	1.9

Table 2. (Continued)

B

NT1200-2011	Depth (mm)	Sedi-BSi Contents (%)	BSi-AR ($g/cm^2/yr$)	Date (Year)		
				Average	Top of Interval	Bottom of Interval
	0	0.8	5.1×10^{-4}	2011.0	2011.5	2010.4
	2	0.8	4.7×10^{-4}	2009.8	2010.4	2009.2
	4	0.9	5.7×10^{-4}	2008.6	2009.2	2008.0
	6	0.8	5.4×10^{-4}	2007.3	2008.0	2006.6
	8	1.1	6.5×10^{-4}	2005.9	2006.6	2005.2
	10	1.3	7.1×10^{-4}	2004.3	2005.2	2003.4
	20	1.2	6.8×10^{-4}	1993.7	1995.9	1991.5
	25	1.4	7.2×10^{-4}	1989.2	1991.5	1986.9
	30	1.1	4.9×10^{-4}	1984.1	1986.9	1981.4
	35	0.9	4.2×10^{-4}	1978.5	1981.4	1975.6
	40	1.3	5.8×10^{-4}	1972.5	1975.6	1969.3
	45	1.4	6.1×10^{-4}	1966.3	1969.3	1963.3
	Avg.	1.1	5.8×10^{-4}			

C

DSH08-2010	Depth (mm)	Sedi-BSi Contents (%)	Mean (%)	STDEV (%)	BSi-AR ($g/cm^2/yr$)	Mean ($g/cm^2/yr$)	STDEV ($g/cm^2/yr$)	Date (Year)
	4	2.42, 2.50	2.46	0.05	20.65×10^{-4}, 21.28×10^{-4}	20.96×10^{-4}	0.45	2010.5
	6	2.30, 2.39	2.34	0.06	21.30×10^{-4}, 22.14×10^{-4}	21.72×10^{-4}	0.59	2009.3
SW01-2012	**Depth (mm)**	**Sedi-BSi Contents (%)**	**Mean (%)**	**STDEV (%)**	**BSi-AR ($g/cm^2/yr$)**	**Mean ($g/cm^2/yr$)**	**STDEV ($g/cm^2/yr$)**	**Date (Year)**
	2	2.68, 2.41	2.54	0.19	16.49×10^{-4}, 14.84×10^{-4}	15.66×10^{-4}	1.16	2006.8
	4	2.17, 2.76	2.46	0.42	13.98×10^{-4}, 17.80×10^{-4}	15.89×10^{-4}	2.70	2005.4

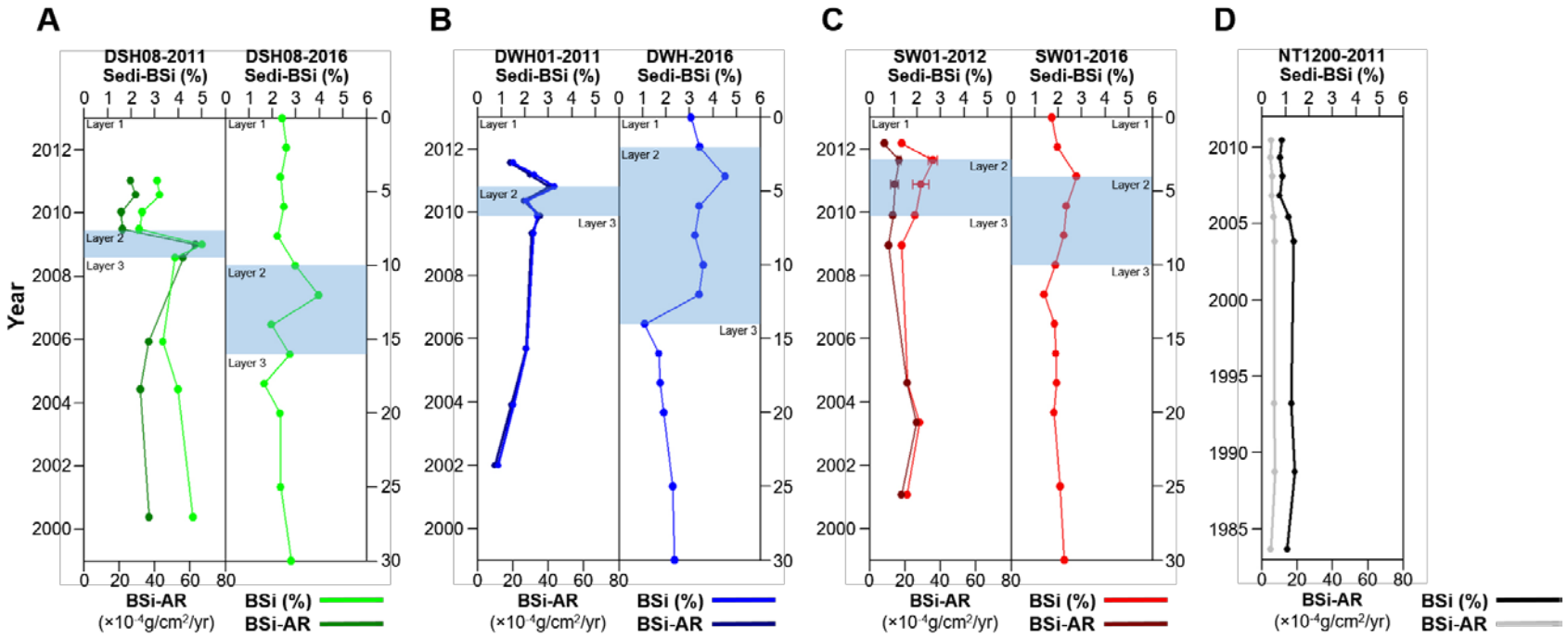

Fig 2. Profiles of Sedi-BSi of each cores. A: 2011 core profile with age (left) and 2016 core profile with core depth (right) from site DSH08, B: 2011 core profile with age (left) and 2016 core profile with core depth (right) from site DWH01, C: 2012 core profile with age (left) and 2016 core profile with core depth (right) from site SW01, D: 2011 core profile with age from site NT1200.

2.4 Discussion

2.4.1 Potential causes for the Sedi-BSi increase during DWH spill.

General comparison with previous records of DWH oil spill

The profiles of Sedi-BSi were consistent with the profiles of the other proxy records previously measured. Fridrik et al., 2016 measured planktic foraminifera accumulation rates from site DSH08 collected in 2011, which increased in the sedimentary interval influenced by the DWH oil spill. Sedi-BSi of the core from site DSH08 collected in 2011 increased similarly in the sedimentary interval influenced by the DWH oil spill (Layer 2). PAH concentrations of cores from sites DSH08 and DSH10 collected in 2010 and 2011 measured by Romero et al. 2015 also increased after the DWH oil spill and corresponded to Sedi-BSi increases after the DWH oil spill at Layer 2 of each core. Site DSH10 is around 18 km south of site DSH08. Radović and Oldenburg et al., in Prep reported that the Dioxy Sulfosuccinate (DOSS) concentration at site DSH08, which is the primary component of the Corexit-9500 dispersant, increased after the DWH oil spill in the same interval. Yan et al., 2016 reported that the number of the diatom frustules caught by the sediment trap deployed at 1,538 meter water depth (~5 km southwest of the DWH platform) in August 25, 2010 were distinctively higher compared to sediment trap data obtained after August 25, 2010. Sites where the sediment traps were deployed were around 7 km southwest of the DWH wellhead. Diatom 16SRNA data of cores from site DSH10 reported by Brooks et al., 2015 showed a consistent trend with the Sedi-BSi profile of cores from site DSH08.

Potential causes for the Sedi-BSi variation in the NGOM

The potential causes for the Sedi-BSi increase are the occurrence of the DWH oil spill and ensuing MOSSFA event according to this study. Sedi-BSi is controlled by variation of surface water primary productivity (Nelson et al., 1995; Tréguer et al., 1995). Environmental

changes have influences on surface water productivity and deposition of its byproducts to the seafloor (Nelson et al., 1995; Tréguer et al., 1995). Diatoms are the most abundant primary producer group in the NGOM (Qian et al., 2003; Strom and Strom, 1996) and diatom frustules from surface water are a dominant source of Sedi-BSi (DeMaster et al., 1996; Nelson et al 1995; Tréguer et al., 1995). The variation of the Sedi-BSi reflects the variation of surface water primary and diatom productivity caused by natural or anthropogenic impacts in the NGOM. Thus, a comprehensive understanding of anthropogenic influences and changed natural environmental inputs is important and necessary to constrain a mechanism for variation of Sedi-BSi after DWH oil spill.

The MOSSFA event is expected to increase the Sedi-BSi after the DWH blowout as an increase in diatom population produces more material to be exported to the seafloor during the MOSSFA event. Increased Sedi-BSi after the DWH spill was derived by surface water diatom blooms. This is supported by the fact that increased primary production was observed through water column chlorophyll fluorescence anomalies measured by optical analysis of satellite imagery (Hu et al., 2011), significantly increased number of the diatom frustules caught by sediment trap at 1,538 m water depth (Yan el al., 2016), and diatom 16S RNA data in sediments in the NGOM (Brooks et al., 2015). This diatom bloom was supported by nutrient input from the Mississippi River (Bianchi et al., 2011; Daly et al., 2016; Lohrenz et al., 1997, 2008; O'Connor et al., 2016; Qian et al., 2003). The DWH spill period coincided with seasonal high discharge period of the Mississippi River (March to April) (Bianchi et al., 2011; Walker et al., 2005). Phytoplankton secreted EPS and TEP as a stress response to oil and dispersant exposure (Daly et al., 2016). These EPS and TEP acted as glue for combining and adsorbing particles in surface water (e.g. diatom frustules, suspended particles, oil residues, dispersants) and formed MOS.

Increased suspended clay-sized minerals combined in the MOS ballasted and made the MOS sink faster than natural marine snow (Daly et al., 2016; Romero et al., 2015; Schwing et al., 2017). Consequently, this caused a more efficient transport and accumulation of diatom frustules on the seafloor.

2.4.2 Preservation of Sedi-BSi

The Sedi-BSi of cores collected in 2016 and prior (2011 to 2012) were compared in order to constrain preservation of increased Sedi-BSi after the DWH oil spill. According to comparison between results of 2016 core and prior, Sedi-BSi in the NGOM are likely to be well preserved. Cores collected in 2016 and previous (2011 to 2012) showed peaks at the DWH oil spill influenced interval (except for NT1200; control site). Higher values of the Sedi-BSi of 2016 and previous cores showed a difference in depth, magnitude of peak, and width of range. It is possible that bioturbation and compaction during sedimentation caused these differences because these processes could change the concentration of the chemistry in sediment. The higher value of Sedi-BSi (DWH) was found at deeper (0 mm to 4 mm) intervals of 2016 cores than cores of 2011 to 2012. The higher Sedi-BSi at the DWH spill influenced interval of cores collected in 2016 were observed in broader depth range (2 mm to 8 mm) than previous cores (2011 to 2012).

Cores collected in 2016 from sites DSH08 and SW01 had the highest peak after the DWH blowout at deeper depth (4 mm, 2 mm respectively) than cores collected in 2011 and 2012. The Sedi-BSi peaks corresponding to DWH in both the 2016 and earlier collections (2011) at site DWH01 were at the same depth (4 mm), but the peak in the 2016 core profile indicated higher values than 2011 (3.26% in 2011 core, 4.51% in 2016 core). The peak at site SW01 collected in 2016 showed similar values with core collected in 2012 (2.54% in 2012 core, 2.78% in 2016

core). The height of peak in profile of the 2016 core from site DSH08 was lower than 2011 (5.01% in 2011 core, 3.97 in 2016 core). The Sedi-BSi of each core was preserved at a similar concentration over 4 to 5 years, demonstrating short-term preservation of DWH spill.

2.4.3 Proxy as an oil spill and the MOSSFA event

This research compared the Sedi-BSi profiles of 2016 cores, prior cores (2011 to 2012), and previously measured proxy records in order to constrain the potentiality of Sedi-BSi as a proxy record for oil spills and ensuing MOSSFA events.

The Sedi-BSi profiles were consistent with previously measured various proxy records of water column and sediment cores from the same and/or proximate sampling sites. PAH, which are recalcitrant and toxic components of petroleum and DOSS, a primary component of the dispersant used during the DWH spill, concentrations were higher in the same age interval (DWH) as the Sedi-BSi profiles. Diatom blooms are related to the amount of freshwater inflow. Diatom blooms are reflected by the increased number of diatom frustules caught by sediment traps deployed in the water column (Yan et al., 2016). These diatom blooms happened in the same period according to the Sedi-BSi profiles. Diatom 16S RNA shows increased values in the DWH spill influenced sedimentary layer (Brooks., et al 2015). EPS reflects the toxicity of the oil and dispersants. EPS, released by phytoplankton and microbial communities as a stress response to petroleum and dispersant exposure, concentration also increased in the same age interval with the Sedi-BSi profiles. With the planktic foraminifera being the consumer group, the fact that planktic foraminifera accumulation rates increase at DWH oil spill influenced sedimentary interval is highly related to diatom blooms and the Sedi-BSi increases during and after DWH oil spill (Fridrik et al., 2016). Integrated interpretation of these previously measured biogeochemical

proxy records supports the occurrence of the MOSSFA event. Thus, using the Sedi-BSi would provide an additional, corroborative tool for measuring the proportion of MOSSFA material that is surface derived and the overall magnitude of the MOSSFA event.

The Sedi-BSi profile is expected to be a useful method to track impact of oil spill and the MOSSFA in long term (geological scale) and short term view. Although preservation of Sedi-BSi in the deep Gulf of Mexico has been not well documented, Sedi-BSi is expected to be well preserved considering environmental conditions. Sedi-BSi is less dissolved at lower temperature and almost perfectly preserved in 5°C (Bidle et al., 2002). DeMaster et al., 1996 reported that higher BSi-AR increase preservation efficiency. Specifically, preservation efficiency is 86% with 31.2×10^{-4} g/cm^2/year and 58% with 7.41×10^{-4} g/cm^2/year. Sedi-BSi with environmental conditions described above has been used to reconstruct paleoproductivity (Bidle et al., 2002). Temperature of the bottom water at this research site measured by CTD was 3.00 °C to 4.97°C (DWH01, 4.13°C; SW01, 3.00°C; DSH08, 4.97°C). BSi-AR measured in this study were 1.5×10^{-4} g/cm^2/year to 6.3×10^{-4} g/cm^2/year at DWH influenced sedimentary intervals. Sedi-BSi should therefore be well preserved in the deep NGOM and the preservation potential of the signal of DWH spill is high. Thus, Sedi-BSi could be used as an archive for DWH oil spill in long term.

Using the Sedi-BSi profile for tracking oil spills and following MOSSFA event also comes with its own limitations. It is hard to observe the consequences of oil spills because sediment extractions can only occur following the accumulation of the Sedi-BSi on the sea floor- a process that varies depending on ocean sedimentation rate. Also, it could be limited to track the consequence of oil spill certain marine environments at certain regions if the dominant primary producer are not diatoms.

2.5 Conclusions

In this research, the MOSSFA event following the DWH was documented by analyzing Sedi-BSi of cores from the NGOM. The potential mechanism for the Sedi-BSi variations in the NGOM and preservation of the Sedi-BSi were constrained. Also, the potential of Sedi-BSi as a proxy record for oil spill and MOSSFA was confirmed.

The profiles of the Sedi-BSi of all cores used in this research except for cores from the site NT1200, control site, indicate commonly increased values at sedimentary intervals influenced by the DWH spill as a consequence of the MOSSFA event. The MOSSFA event caused the surface material with an increased diatom population to be transported and accumulated efficiently to the seafloor during the DWH oil spill. Thus, Sed-BSi would be increased after the DWH oil spill. It is found that increased Sedi-BSi was well preserved through comparing profiles of cores collected in 2016 and prior (2010 ~ 2012). Position, magnitude, and width of depth ranges of higher Sedi-BSi contents in profiles of 2016 cores indicate different compared to previous cores.

The Sedi-BSi would be a useful and effective proxy for oil spills and ensuing MOSSFA event according to integrative perspectives of this research. The variations in the Sedi-BSi trends are consistent with various previously measured proxy records (planktic foraminifera, PAH, DOSS, EPS, diatom 16S RNA, and diatom frustules collected in sediment trap in water column) of water column and sediment cores. These proxies represent serial events and phenomena including oil spilling, applied dispersant, diatom blooming which are the component of the MOSSFA event. Thus, the Sedi-BSi could give a comprehensive perspective to understand oil spill and following MOSSFA event.

2.6 References

Alldredge, A.L. and Silver, M.W., 1988. Characteristics, dynamics and significance of marine snow. *Progress in oceanography*, *20*(1), pp.41-82.

Appleby, P.G. and Oldfieldz, F., 1983. The assessment of 210Pb data from sites with varying sediment accumulation rates. *Hydrobiologia*, *103*(1), pp.29-35.

Atlas, R.M. and Hazen, T.C., 2011. Oil biodegradation and bioremediation: a tale of the two worst spills in US history.

Baguley, J.G., Montagna, P.A., Cooksey, C., Hyland, J.L., Bang, H.W., Morrison, C., Kamikawa, A., Bennetts, P., Saiyo, G., Parsons, E. and Herdener, M., 2015. Community response of deep-sea soft-sediment metazoan meiofauna to the Deepwater Horizon blowout and oil spill. *Marine Ecology Progress Series*, *528*, pp.127-140.

Bianchi, T.S., Cook, R.L., Perdue, E.M., Kolic, P.E., Green, N., Zhang, Y., Smith, R.W., Kolker, A.S., Ameen, A., King, G. and Ojwang, L.M., 2011. Impacts of diverted freshwater on dissolved organic matter and microbial communities in Barataria Bay, Louisiana, USA. *Marine environmental research*, *72*(5), pp.248-257.

Bidle, K.D., Manganelli, M. and Azam, F., 2002. Regulation of oceanic silicon and carbon preservation by temperature control on bacteria. *Science*, *298*(5600), pp.1980-1984.

Binford, M.W., 1990. Calculation and uncertainty analysis of 210 Pb dates for PIRLA project lake sediment cores. *Journal of Paleolimnology*, *3*(3), pp.253-267.

Brooks, G.R., Larson, R.A., Schwing, P.T., Romero, I., Moore, C., Reichart, G.J., Jilbert, T., Chanton, J.P., Hastings, D.W., Overholt, W.A. and Marks, K.P., 2015. Sedimentation pulse in the NE Gulf of Mexico following the 2010 DWH blowout. *PLoS One*, *10*(7), p.e0132341.

Daly, K.L., Passow, U., Chanton, J. and Hollander, D., 2016. Assessing the impacts of oil-associated marine snow formation and sedimentation during and after the Deepwater Horizon oil spill. *Anthropocene*, *13*, pp.18-33.

DeMaster, D.J., 1981. The supply and accumulation of silica in the marine environment. *Geochimica et Cosmochimica acta*, *45*(10), pp.1715-1732.

DeMaster, D.J., Ragueneau, O. and Nittrouer, C.A., 1996. Preservation efficiencies and accumulation rates for biogenic silica and organic C, N, and P in high-latitude sediments: The Ross Sea. *Journal of Geophysical Research: Oceans*, *101*(C8), pp.18501-18518.

Fridrik EE, Schwing PT, Ramirez H, Larson RA, Brooks GR, O'Malley BJ, Hollander DJ. Comparative Records of Planktic Foraminiferal Mass Accumulation Rates Following the DWH and IXTOC Events. In Proceedings of the Gulf of Mexico Oil Spill and Ecosystem Science Conference, Tampa, FL, 2016.

Guidi, L., Gorsky, G., Claustre, H., Miquel, J.C., Picheral, M. and Stemmann, L., 2008. Distribution and fluxes of aggregates> 100 μm in the upper kilometer of the South-Eastern Pacific. *Biogeosciences*, *5*(5), pp.1361-1372.

Gutierrez, T., Berry, D., Yang, T., Mishamandani, S., McKay, L., Teske, A. and Aitken, M.D., 2013. Role of bacterial exopolysaccharides (EPS) in the fate of the oil released during the Deepwater Horizon oil spill. *PloS one*, *8*(6), p.e67717.

Hastings, D.W., Schwing, P.T., Brooks, G.R., Larson, R.A., Morford, J.L., Roeder, T., Quinn, K.A., Bartlett, T., Romero, I.C. and Hollander, D.J., 2016. Changes in sediment redox conditions following the BP DWH blowout event. *Deep Sea Research Part II: Topical Studies in Oceanography*, *129*, pp.167-178.

Hu, C., Weisberg, R.H., Liu, Y., Zheng, L., Daly, K.L., English, D.C., Zhao, J. and Vargo, G.A., 2011. Did the northeastern Gulf of Mexico become greener after the Deepwater Horizon oil spill?. *Geophysical Research Letters*, *38*(9).

Jochens, A.E., 2002. Northeastern Gulf of Mexico chemical oceanography and hydrography study [microform].

Kujawinski, E.B., Kido Soule, M.C., Valentine, D.L., Boysen, A.K., Longnecker, K. and Redmond, M.C., 2011. Fate of dispersants associated with the Deepwater Horizon oil spill. *Environmental science & technology*, *45*(4), pp.1298-1306.

Lohrenz, S.E., Fahnenstiel, G.L., Redalje, D.G., Lang, G.A., Chen, X. and Dagg, M.J., 1997. Variations in primary production of northern Gulf of Mexico continental shelf waters linked to nutrient inputs from the Mississippi River. *Marine Ecology Progress Series*, *155*, pp.45-54.

Lohrenz, S.E., Redalje, D.G., Cai, W.J., Acker, J. and Dagg, M., 2008. A retrospective analysis of nutrients and phytoplankton productivity in the Mississippi River plume. *Continental Shelf Research*, *28*(12), pp.1466-1475.

McNutt, M.K., Camilli, R., Guthrie, G.D., Hsieh, P.A., Labson, V.F., Lehr, W.J., Maclay, D., Ratzel, A.C. and Sogge, M.K., 2011. *Assessment of flow rate estimates for the Deepwater Horizon/Macondo well oil spill*. US Department of the Interior.

Montagna, P.A., Baguley, J.G., Cooksey, C., Hartwell, I., Hyde, L.J., Hyland, J.L., Kalke, R.D., Kracker, L.M., Reuscher, M. and Rhodes, A.C., 2013. Deep-sea benthic footprint of the Deepwater Horizon blowout. *PloS one*, *8*(8), p.e70540.

Murawski, S.A., Fleeger, J.W., Patterson III, W.F., Hu, C., Daly, K., Romero, I. and Toro-Farmer, G.A., 2016. How Did the Oil Spill Affect Coastal and Continental Deepwater Horizon Shelf Ecosystems of the Gulf of Mexico?. *Oceanography*, *29*(3), pp.160-173.

Nelson, D.M., Tréguer, P., Brzezinski, M.A., Leynaert, A. and Quéguiner, B., 1995. Production and dissolution of biogenic silica in the ocean: revised global estimates, comparison with regional data and relationship to biogenic sedimentation. *Global Biogeochemical Cycles*, *9*(3), pp.359-372.

O'Connor, B.S., Muller-Karger, F.E., Nero, R.W., Hu, C. and Peebles, E.B., 2016. The role of Mississippi River discharge in offshore phytoplankton blooming in the northeastern Gulf of Mexico during August 2010. *Remote sensing of environment*, *173*, pp.133-144.

Passow, U., Ziervogel, K., Asper, V. and Diercks, A., 2012. Marine snow formation in the aftermath of the Deepwater Horizon oil spill in the Gulf of Mexico. *Environmental Research Letters*, *7*(3), p.035301.

Passow, U. and Ziervogel, K., 2016. Marine snow sedimented oil released during the Deepwater Horizon spill. *Oceanography*, *29*(3), pp.118-125.

Qian, Y., Jochens, A.E., Kennicutt Ii, M.C. and Biggs, D.C., 2003. Spatial and temporal variability of phytoplankton biomass and community structure over the continental margin of the northeast Gulf of Mexico based on pigment analysis. *Continental Shelf Research*, *23*(1), pp.1-17.

Rabalais, N.N., Turner, R.E., Gupta, B.K.S., Platon, E. and Parsons, M.L., 2007. Sediments tell the history of eutrophication and hypoxia in the northern Gulf of Mexico. *Ecological Applications*, *17*(sp5), pp.S129-S143.

Romero, I.C., Schwing, P.T., Brooks, G.R., Larson, R.A., Hastings, D.W., Ellis, G., Goddard, E.A. and Hollander, D.J., 2015. Hydrocarbons in deep-sea sediments following the 2010 Deepwater Horizon blowout in the northeast Gulf of Mexico. *PLoS One*, *10*(5), p.e0128371.

Romero, I.C., Toro-Farmer, G., Diercks, A.R., Schwing, P., Muller-Karger, F., Murawski, S. and Hollander, D.J., 2017. Large-scale deposition of weathered oil in the Gulf of Mexico following a deep-water oil spill. *Environmental pollution*, *228*, pp.179-189.

Schwing, P.T., Romero, I.C., Brooks, G.R., Hastings, D.W., Larson, R.A. and Hollander, D.J., 2015. A decline in benthic foraminifera following the Deepwater Horizon event in the northeastern Gulf of Mexico. *PLoS One*, *10*(3), p.e0120565.

Schwing, P.T., Romero, I.C., Larson, R.A., O'Malley, B.J., Fridrik, E.E., Goddard, E.A., Brooks, G.R., Hastings, D.W., Rosenheim, B.E., Hollander, D.J. and Grant, G., 2016. Sediment core extrusion method at millimeter resolution using a calibrated, threaded-rod. *Journal of visualized experiments: JoVE*, (114).

Schwing, P.T., Brooks, G.R., Larson, R.A., Holmes, C.W., O'Malley, B.J. and Hollander, D.J., 2017. Constraining the Spatial Extent of Marine Oil Snow Sedimentation and Flocculent Accumulation Following the Deepwater Horizon Event Using an Excess 210Pb Flux Approach. *Environmental Science & Technology*, *51*(11), pp.5962-5968.

Strom, S.L. and Strom, M.W., 1996. Microplankton growth, grazing, and community structure in the northern Gulf of Mexico. *Marine Ecology Progress Series*, *130*, pp.229-240.

Treguer, P., Nelson, D.M., Van Bennekom, A.J., DeMaster, D.J., Leynaert, A. and Quéguiner, B., 1995. The silica balance in the world ocean: a reestimate. *Science*, *268*(5209), pp.375-379.

US Department of Interior. (2010, August 02). U.S. scientific teams refine estimates of oilflow from BP's well prior to capping. Retrieved December 16, 2010, from http://www.doi.gov/news/pressreleases/US-Scientific-Teams-Refine-Estimates-of-Oil-Flow-from-BP-Well-Prior-to-Capping.cfm.

Walker, N.D., Wiseman Jr, W.J., Rouse Jr, L.J. and Babin, A., 2005. Effects of river discharge, wind stress, and slope eddies on circulation and the satellite-observed structure of the Mississippi River plume. *Journal of Coastal Research*, pp.1228-1244.

Wei, C.L., Rowe, G.T., Hubbard, G.F., Scheltema, A.H., Wilson, G.D., Petrescu, I., Foster, J.M., Wicksten, M.K., Chen, M., Davenport, R. and Soliman, Y., 2010. Bathymetric zonation of deep-sea macrofauna in relation to export of surface phytoplankton production. *Marine Ecology Progress Series*, *399*, pp.1-14.

Yan, B., Passow, U., Chanton, J.P., Nöthig, E.M., Asper, V., Sweet, J., Pitiranggon, M., Diercks, A. and Pak, D., 2016. Sustained deposition of contaminants from the Deepwater Horizon spill. *Proceedings of the National Academy of Sciences*, *113*(24), pp.E3332-E3340.

Chapter 3

Variation of Sedimentary Biogenic Silica Deposition in the Southern Gulf of Mexico related to the IXTOC-I Oil Spill (1979-80) and other influences

Abstract

The primary goal of this research is constraining the impact of the IXTOC-I oil spill event (1979-1980) and anthropogenic influences (e.g. dam constructions) on surface water primary productivity in the Southern Gulf of Mexico. A secondary goal was to compare the consequence of two massive oil spills [IXTOC-I and Deepwater Horizon (DWH)] and the associated Marine Oil Snow Sedimentation Flocculent Accumulation (MOSSFA). For this, sedimentary biogenic silica (Sedi-BSi) was measured in cores collected from the Bay of Campeche in the southern Gulf of Mexico (SGOM, IXTOC-I) and from the northern Gulf of Mexico (NGOM, DWH) that were dated using short-lived radioisotope (i.e. $^{210}Pb_{xs}$) age models. Sedi-BSi provides an independent record of the surface derived portion of MOSSFA inputs as a proxy of surface water primary productivity (e.g. diatom blooms). The IXTOC-I oil spill (1970-1980) was one of the largest oil spills in history and it is likely that a MOSSFA event occurred as a direct result. Only one core (of three from oil spill area utilized in this study), collected 81 km from the IXTOC-I wellhead, had elevated levels of Sedi-BSi content in the sedimentary interval associated with IXTOC-I. However, Sedi-BSi was elevated in sedimentary intervals influenced by DWH spill in every core collected from the NGOM (except for control site) influenced by the

DWH spill. The down-core profiles of Sedi-BSi from the other cores collected in the SGOM are consistent with history of dam construction (1949 to 1989) on the Grijalva and Papaloapan river systems. These two river systems are the dominant freshwater and nutrient sources for primary production in the Bay of Campeche region and therefore the dominant control on diatom productivity and Sedi-BSi distribution. Consequently, distribution of annual fresh water outflow and nutrient supply has transitioned from seasonal and highly variable (before 1940's) to stable (after 1980's). Overall, Sedi-BSi provides an independent record of surface derived MOSSFA inputs and serves a proxy for other anthropogenic influences related to surface primary productivity variability.

3.1 Introduction

In this study, the sedimentary biogenic silica (Sedi-BSi) of sediments cores from the Bay of Campeche in the southern Gulf of Mexico (SGOM) were analyzed to track potential factors that can alter primary productivity such as the 1979-80 IXTOC-I oil spill and dam constructions. Variations of Sedi-BSi were observed after the dam constructions on the Grijalva-Usumacinta, the Papaloapan river systems, and the IXTOC-I blowout.

Sedi-BSi reflects diatom surface water productivity as their frustules sink after death. Primary productivity is highly influenced by environmental change, whether that be natural or anthropogenic. These environmental changes can be documented by measuring Sedi-BSi (Nelson et al., 1995; Tréguer et al., 1995). Studying Sedi-BSi provides important information about diatom productivity, the largest primary producer group in the SGOM (Hernández-Becerril et al., 2008; Licea et al., 2011).

Primary productivity in the SGOM, including the Bay of Campeche, is controlled by various natural and anthropogenic factors including variations of river water discharge rates, upwelling by wind stress, seasonal current direction shifts, long and short term natural impacts, and constructions on rivers (Gómez, 2002; Martínez-López and Zavala-Hidalgo, 2009; Ruiz-Fernández et al., 2012; Salmeron-Garcia et al., 2011; Zavala-Hidalgo et al., 2003; Zavala-Hidalgo et al., 2006). The three rivers that provide majority of freshwater and nutrient sources to the Bay of Campeche are the Grijalva-Usumacinta, Papaloapan, and Coatzacoalcos River (Gracia et al., 2013; Jernelöv and Lindén, 1981; Kemp et al., 2016; Martínez-López and Zavala-Hidalgo, 2009; Salmerón-García et al., 2011).

Surface currents (e.g. the Loop current, the along-cost current, and the Cross-shelf transport) affect the primary productivity of the SGOM. Surface water masses are controlled by two surface currents in the Bay of Campeche in the SGOM: the Loop Current and the Along-Coast current (also known as the Along-Shelf Current) (Dubranna et al., 2011; Martínez-López and Zavala-Hidalgo, 2009). The Loop Current is the predominant surface current outside of shelf area (Dubranna et al., 2011; Martínez-López and Zavala-Hidalgo, 2009; Salmeron-Garcia et al., 2011). The along-coast currents are dominant on the surface water over the shelf area (Martínez-López and Zavala-Hidalgo, 2009; Morey et al, 2005; Salmeron-Garcia et al., 2011; Zavala-Hidalgo et al., 2003; Zavala-Hidalgo et al., 2006; Zavala-Hidalgo et al., 2014). The Cross-shelf transport is the most important mechanisms of laterally transporting surface water masses on the shelf to surface water over the deep ocean (Martínez-López and Zavala-Hidalgo, 2009; Morey et al, 2005; Salmeron-Garcia et al., 2011; Zavala-Hidalgo et al., 2003; Zavala-Hidalgo et al., 2006; Zavala-Hidalgo et al., 2014). The Cross-shelf transport redistributes and transports nutrients contained in surface water mass over the continental shelf area, originating from river mouths

and deep sea upwelling, from the continental shelf to the deep ocean (Martínez-López and Zavala-Hidalgo, 2009; Morey et al, 2005; Salmeron-Garcia et al., 2011; Zavala-Hidalgo et al., 2003; Zavala-Hidalgo et al., 2006; Zavala-Hidalgo et al., 2014). The Cross-shelf transport is formed seasonally in the Bay of the Campeche by confluence of the along-coast current from west to east (down-coast) and from east to west (up-coast) (Martínez-López and Zavala-Hidalgo, 2009; Morey et al, 2005; Salmeron-Garcia et al., 2011; Zavala-Hidalgo et al., 2003; Zavala-Hidalgo et al., 2006; Zavala-Hidalgo et al., 2014). Primary productivity on the outer shelf is highly influenced by formation of the Cross-shelf transport (Martínez-López and Zavala-Hidalgo, 2009; Morey et al, 2005; Salmerón-García et al., 2011). There is less fluctuation of primary production on the SGOM continental shelf seasonally compared to the outer shelf (Martínez-López and Zavala-Hidalgo, 2009; Salmerón-García et al., 2011; Zavala-Hidalgo et al., 2006; Zavala-Hidalgo et al., 2014).

The IXTOC-I blowout occurred in June 1979 at a water depth of 50 m in the Bay of Campeche and spilled 130 million US gal of the oil over a span of 10 months (Farrington, 1980; Jernelöv and Lindén, 1981). Dispersant (Corexit 9527) was applied on the oil spill area by air (Boehm and Flest, 1982; Farrington, 1980; Jernelöv and Lindén, 1981). Due to prevailing currents, spilled oil was transported northwest from June-August of 1979 (Boehm and Flest, 1982; Farrington, 1980). High oil concentrations were observed in a triangle-shaped area with apexes at the IXTOC-I wellhead, Veracruz, and Cabo Rojo in Mexico (Boehm and Flest, 1982; Farrington, 1980). Seasonal current shifts decreased spilled oil observed in the triangle area with higher amounts of surface oil in the northeast, east and southeast of the blowout site and only a small amount of oil west of the wellhead (Boehm and Flest, 1982; Farrington, 1980).

According to this research, dam constructions on the Grijalva and Papaloapan river systems affect annual and seasonal productivity of the research area. Dam construction on these river systems began after 1940 to minimize flood damage through the control of the discharge rates of these two rivers (Fabian Rivera-Trejo et al., 2010; Marengo, Athie & Calahorra, 2006; Sonnenfeld, 1992). The dam construction stabilized river water discharge rates and the amount of nutrient input (Fabian Rivera-Trejo et al., 2010; Lázaro-Vázquez et al., 2018; Marengo, Athie & Calahorra, 2006; Papaloapan Ref).

Analyzing Sedi-BSi profiles allows for potential mechanisms that influence diatom production to be determined post IXTOC-I oil spill in the Bay of Campeche area and the potential for a subsequent MOSSFA event. The Sedi-BSi variation and surrounding environmental conditions influenced by the IXTOC-I oil spill in SGOM and the 2010 Deepwater Horizon (DWH) oil spill in the northern Gulf of Mexico (NGOM) were compared in order to characterize correlation between massive oil spills and the MOSSFA event. Sedi-BSi profiles also vary with dam constructions. The dam construction period and Sedi-BSi profiles were compared in combination with other natural variation (e.g. river discharge rate, sea surface current) to constrain potential mechanisms for effects of dam construction on diatom production.

3.2 Methods

Field Sampling

Three sediment cores were collected from three sites (IXW750A, IXW250A, IXN750) using an Oktopus MC-08-12 multicoring system during the Center for Integrated Modeling and Analysis of Gulf Ecosystems (C-IMAGE) cruises in August 2015 (Fig 3A, Table 3A). IXW750A and IXN750 located on outer continental shelf. IXW250A is located on shelf area.

Seven sediment cores were collected from four sites (DWH01, SW01, DSH08, and NT1200) using an MC-800 multicorer during the C-IMAGE cruises from December 2011 to September 2016 (Fig 2D, Table 2B). Site DWH01 is located near (<1km) the DWH wellhead. NT1200 is located 250 km away from the blowout site and didn't showed increasing hydrocarbon concentrations both of surface and subsurface plume related to DWH oil spill l (DSH08, 70 km; SW01, 87 km). Thus, site NT1200 is used as control site (Fig 3B, Table 3B).

Cores were sub-sampled by extrusion at 2-5 mm intervals using a calibrated, threaded-rod extrusion device (Schwing et al., 2016) in order to conduct analysis for measuring various proxies including planktonic foraminiferal tests, biomarkers, grain size, and residues of the oil and dispersant. Extruded and sliced subsamples were freeze dried, ground, and homogenized to measure Sedi-BSi contents and BSi accumulation rates (BSi-AR).

Sedi-BSi Analysis

Sedi-BSi was measured by using a wet alkaline extraction method modified from DeMaster (1981). This method is described in "2.2 Method – Sedi-BSi Analysis" section in the chapter 2.

Chronology

Chronology was dated using short-lived radioisotope analysis to identify pre-, during, and post the Deepwater Horizon and IXTOC-I oil spill (Brooks et al, 2015; Schwing et al., 2017). In formations about the chronology analysis is documented in "2.2 Method – Chronology" section in the chapter 2.

Data Uncertainty

Three samples from the 2010 core at site DSH08 and two samples from the 2012 core at site SW01 were used to constrain data uncertainty of Sedi-BSi. Information about the data uncertainty is described in the "2.2 Method – Data Uncertainty" section in the chapter 2 (Table 2C).

Table 3. A: Location and depth of coring sites in the SGOM and collection date. B: Location and depth of coring sites in the NGOM and collection date.

A

SGOM	Latitude	Longitude	Water Depth (m)	Collection Date
IXW750A	19° 27.52 N	94° 35.15 W	1,474	08/05/2015
IXW250A	19° 25.79 N	93° 05.68 W	583	08/06/2015
IXN750	20° 10.20 N	92° 25.20 W	1,647	08/03/2015

B

NGOM	Latitude	Longitude	Water Depth (m)	Collection Date
DSH08-2010	29° 07.93 N	87° 52.00 W	1,100	12/05/2010
DWH01-2011	28° 44.74 N	88° 22.87 W	1,550	09/23/2011
SW01-2012	28° 14.34 N	89° 07.89 W	1,131	04/09/2012
NT1200-2011	27° 57.98 N	86° 01.39 W	1,200	06/27/2011
DSH08-2016	29° 07.25 N	87° 52.08 W	1,130	09/09/2016
DWH01-2016	28° 43.51 N	88° 23.24 W	1,577	09/08/2016
SW01-2016	28° 14.42 N	89° 07.30 W	1,132	09/08/2016

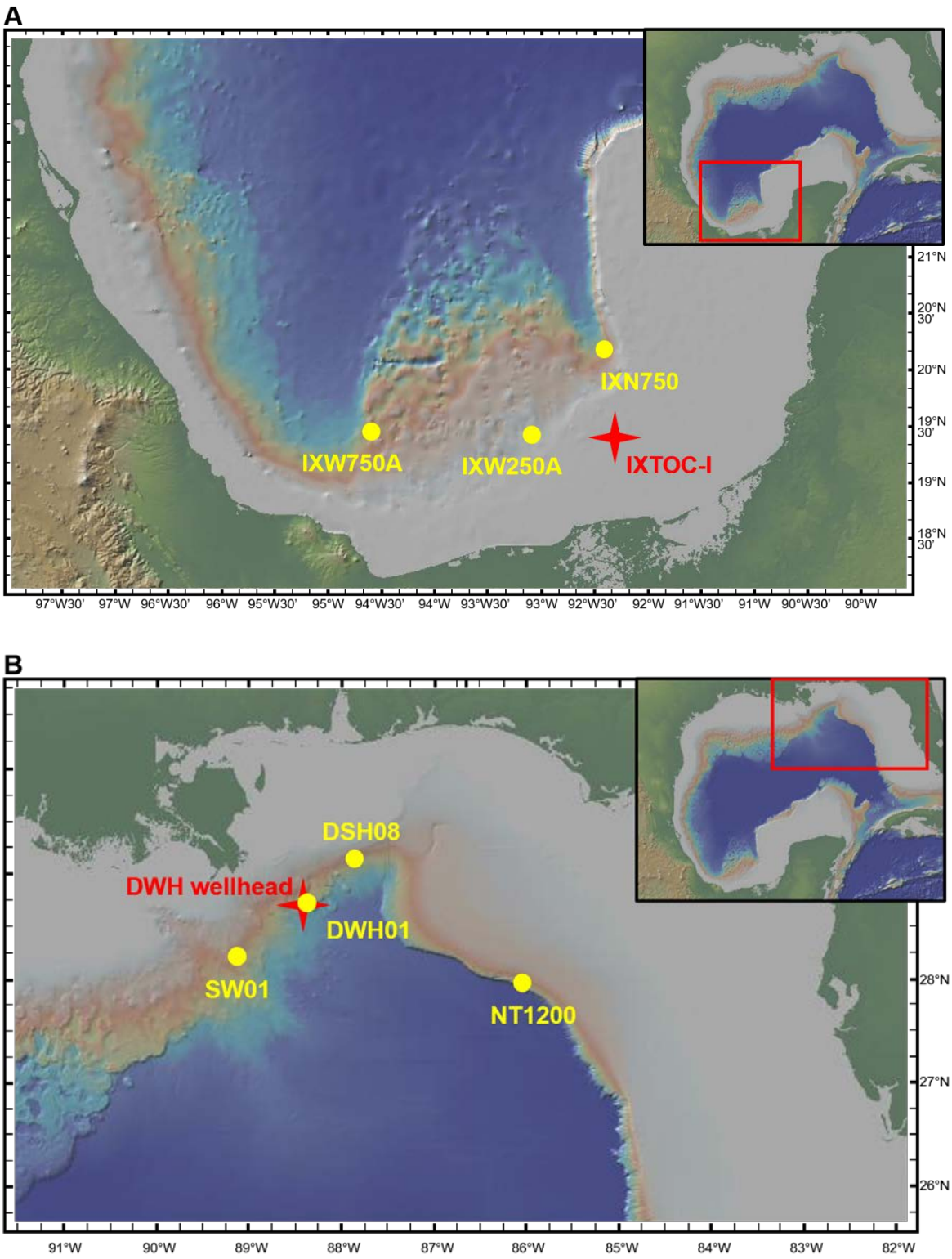

Fig 3. A: Coring sites in the SGOM and location of the IXTOC-I blowout site. B: Coring sites in the NGOM and location of the DWH wellhead.

3.3 Results

The SGOM

Each profile of cores was sectionalized based on the variation of Sedi-BSi (Table 3A-3C, Fig 4)

Site IXW750A

The increases of Sedi-BSi contents and BSi-AR from 20-24 mm (1981 to 1986) ranged from 1.1% to 2.4% (a 117.4% increase) and 3.8×10^{-4} g/cm^2/year to 7.8×10^{-4} g/cm^2/year (a 104.5% increases). These increases were consistent with Peñitas dam construction on the Grijalva river system (1979 to 1986). This was 24.1% (Sedi-BSi contents) and 8.2% (BSi-AR) higher than the baseline average (32-56 mm, before 1970). The baseline average was 1.9% ($\pm 0.2\%$) and 7.2×10^{-4} g/cm^2/year ($\pm 0.7 \times 10^{-4}$ g/cm^2/year) for Sedi-BSi contents and BSi-AR respectively (Table 3A, Fig 4B).

An increase in Sedi-BSi was also observed at 32-28 mm (1970 to 1976) and average of Sedi-BSi is 2.3% ($\pm 0.6\%$) and average of BSi-AR is 8.6×10^{-4} g/cm^2/year ($\pm 2.3 \times 10^{-4}$ g/cm^2/year). These increases are matched with the Angostura dam construction on the Grijalva River (1969 to 1974). Sedi-BSi contents increased from 1.7% to 2.7% (a 58.9% increases) and BSi-AR was increased from 6.3×10^{-4} g/cm^2/year to 10.9×10^{-4} g/cm^2/year (a 72.2% increase). There were also increases of 39.8% in Sedi-BSi contents and 51.8% in BSi-AR compared to an average of baseline, below 32 mm and before 1970 respectively (Table 3A, Fig 4B).

Sedi-BSi contents and BSi-AR decreased from 2.7% to 1.1% (a 59.2% decrease) and from 8.6×10^{-4} g/cm^2/year to 3.8×10^{-4} g/cm^2/year (a 56.0% decrease) at 28-24 mm (1976 to 1981). These decreases were matched with the construction of the Cerro de Oro dam on the Papaloapan river system (1973 to 1989). There was 42.9% and 47.1% decline comparing to

average of baseline from 32-56 mm of Sedi-BSi contents and BSi-AR respectively (below 32 mm, before 1970). It was 58.8% and 55.9% lower than the average of 32-28 mm, the high Sedi-BSi layer, for Sedi-BSi contents and BSi-AR respectively (Table 3A, Fig 4B).

Site IXN750

Variation in Sedi-BSi contents and BSi-AR in sediment core from site IXN750 also showed a correlation with dam constructions. This core showed relatively lower values of Sedi-BSi contents and BSi-AR at 38-20 mm (1968 to 1989). These decreases were matched with sequential construction of three dams (the Angostrura, Chicoasén, and Peñitas dams) on the Grijalva river system during 1969 to 1986. The average Sedi-BSi contents and BSi-AR in this sedimentary interval were 1.6% ($\pm$0.4%) and 5.7×10^{-4} g/cm^2/year ($\pm1.4\times10^{-4}$ g/cm^2/year). This was 22.9% and 34.2% decline of Sedi-BSi contents and BSi-AR compared to values before the dam constructions, baseline (40-90 mm; 1927 to 1965). Baseline average of Sedi-BSi contents is 2.0% ($\pm$0.2%) and average of BSi-AR is 8.6×10^{-4} g/cm^2/year ($\pm1.3\times10^{-4}$ g/cm^2/year). Compared to an average of baseline value (Layer 3, 40-90 mm), the minimum value of the low Sedi-BSi layer indicates 42.9% and 48.8% decreases of Sedi-BSi contents and BSi-AR respectively (Table 3B, Fig 4C).

Site IXW250A

A peak of Sedi-BSi was found at IXTOC-I oil spill influenced intervals (48-52 mm, 1976 to 1981). Sedi-BSi contetns and BSi-AR increased from 0.7% to 2.2% (a 245.1% increase) and from 4.1×10^{-4} g/cm^2/year to 15.2×10^{-4} g/cm^2/year (a 269.0 % increase) respectively. The Sedi-BSi contents and BSi-AR were decreased at 52-54 mm, (1974 to 1976). Sedi-BSi contents and

BSi-AR were decreased from 1.9% to 0.7% (a 65.00% decrease) and from 12.6×10^{-4} g/cm^2/year to 4.1×10^{-4} g/cm^2/year (a 67.4% decrease) respectively. This decline correlates with the Angostura dam construction (1969 to 1974) which is the dam with the biggest reservoir capacity among the Grijalva river system dams (Table 3C, Fig 4A).

The NGOM

The results of Sedi-BSi measurements from the research site cores in the NGOM and sub-layered core information are documented in "2.3 Results" section in Chapter 2 with Table 2 and Fig 2. Every profiles of cores (except core from site NT1200; control site) was distinguished by 3 sub layer (Layer 1, Post-DWH; Layer 2, DWH; Layer 3, Pre-DWH) based on chronology and the variation of Sedi-BSi. Increased Sedi-BSi after the DWH blowout were found in every core except for core NT1200, which was the control site

Table 4. Sedi-BSi with depth and chronology for each cores from the NGOM and SGOM.

A. IXW750A

Depth (mm)	Sedi-BSi Contents (%)	BSi-AR ($g/cm^2/yr$)	Date (Year)		
			Average	Top of Interval	Bottom of Interval
0	1.5	3.5×10^{-4}	2012.2	2015.6	2008.7
5	2.2	5.3×10^{-4}	2004.0	2008.7	1999.2
10	1.6	4.8×10^{-4}	1997.0	1999.2	1994.8
15	2.2	6.8×10^{-4}	1991.0	1994.8	1987.1
20	2.4	7.8×10^{-4}	1985.8	1987.1	1984.5
22	1.5	4.4×10^{-4}	1983.3	1984.5	1982.2
24	1.1	3.8×10^{-4}	1980.8	1982.2	1979.5
26	2.3	7.4×10^{-4}	1978.2	1979.5	1976.9
28	2.7	8.6×10^{-4}	1975.7	1976.9	1974.5
30	2.6	10.9×10^{-4}	1973.0	1974.5	1971.5
32	1.7	6.3×10^{-4}	1970.3	1971.5	1969.0
34	1.8	6.5×10^{-4}	1967.3	1969.0	1965.6
36	2.0	7.4×10^{-4}	1964.5	1965.6	1963.3
38	2.1	8.2×10^{-4}	1961.6	1963.3	1959.9
40	2.1	7.6×10^{-4}	1959.0	1959.9	1958.0
44	1.9	7.2×10^{-4}	1954.7	1955.9	1953.4
46	2.0	7.3×10^{-4}	1951.9	1953.4	1950.3
48	2.1	7.9×10^{-4}	1949.0	1950.3	1947.8
50	1.9	7.4×10^{-4}	1945.8	1947.8	1943.8
54	1.6	5.8×10^{-4}	1937.3	1938.8	1935.7
56	1.9	7.4×10^{-4}	1933.6	1935.7	1931.6
Avg.	2.0	6.8×10^{-4}			

B. IXN750

Depth (mm)	Sedi-BSi Contents (%)	BSi-AR ($g/cm^2/yr$)	Date (Year)		
			Average	Top of Interval	Bottom of Interval
0	1.5	4.2×10^{-4}	2012.4	2015.6	2009.2
5	2.5	7.5×10^{-4}	2005.6	2009.2	2002.0
10	2.0	6.2×10^{-4}	1999.1	2002.0	1996.3
15	1.5	5.0×10^{-4}	1993.4	1996.3	1990.6
20	1.3	4.4×10^{-4}	1989.4	1990.6	1988.2
22	1.3	4.7×10^{-4}	1987.1	1988.2	1986.1
24	2.1	8.0×10^{-4}	1984.9	1986.1	1983.8
26	1.6	6.2×10^{-4}	1982.5	1983.8	1981.2
28	1.4	5.3×10^{-4}	1979.9	1981.2	1978.6
30	2.1	7.7×10^{-4}	1977.3	1978.6	1976.0
32	1.2	4.6×10^{-4}	1974.8	1976.0	1973.6
34	1.9	6.6×10^{-4}	1972.3	1973.6	1971.0
36	1.3	4.5×10^{-4}	1969.8	1971.0	1968.6
38	1.3	4.9×10^{-4}	1967.6	1968.6	1966.7
40	2.1	8.2×10^{-4}	1965.7	1966.7	1964.7
44	2.0	7.3×10^{-4}	1962.1	1962.9	1961.3
48	2.1	8.3×10^{-4}	1958.8	1959.5	1958.0
54	1.9	8.1×10^{-4}	1954.6	1955.3	1953.8
58	2.0	8.9×10^{-4}	1951.8	1952.5	1951.0
62	1.9	7.2×10^{-4}	1949.1	1949.7	1948.5
68	2.4	9.2×10^{-4}	1945.2	1945.7	1944.6
74	1.8	8.7×10^{-4}	1941.7	1942.3	1941.0
80	2.0	9.5×10^{-4}	1937.7	1938.4	1937.0
85	1.6	7.8×10^{-4}	1932.5	1934.7	1930.2
90	2.4	11.9×10^{-4}	1927.6	1930.2	1924.9
Avg.	1.8	1.8×10^{-4}			

Table 4. (Continued)

C. IXW250A

Depth (mm)	Sedi-BSi Contents (%)	BSi-AR ($g/cm^2/yr$)	Date (Year)		
			Average	Top of Interval	Bottom of Interval
0	1.3	8.9×10^{-4}	2015.2	2015.6	2014.7
5	1.8	17.6×10^{-4}	2014.0	2014.7	2013.2
10	2.1	25.6×10^{-4}	2012.1	2013.2	2010.9
15	1.9	21.9×10^{-4}	2009.5	2010.9	2008.0
20	1.6	16.6×10^{-4}	2007.4	2008.0	2006.8
22	1.5	14.5×10^{-4}	2006.2	2006.8	2005.5
24	1.5	15.8×10^{-4}	2004.8	2005.5	2004.0
26	1.6	14.5×10^{-4}	2003.3	2004.0	2002.5
28	1.6	14.0×10^{-4}	2001.8	2002.5	2001.0
30	2.2	19.7×10^{-4}	2000.2	2001.0	1999.3
32	1.8	15.5×10^{-4}	1998.6	1999.3	1997.8
34	1.9	16.0×10^{-4}	1996.9	1997.8	1996.0
36	1.4	11.8×10^{-4}	1995.1	1996.0	1994.1
38	1.9	14.3×10^{-4}	1993.1	1994.1	1992.0
40	1.3	8.8×10^{-4}	1990.9	1992.0	1989.7
42	1.9	13.6×10^{-4}	1988.4	1989.7	1987.1
44	1.1	7.5×10^{-4}	1985.8	1987.1	1984.5
46	1.7	10.9×10^{-4}	1983.2	1984.5	1982.0
48	2.2	15.2×10^{-4}	1980.9	1982.0	1979.7
50	2.2	12.3×10^{-4}	1978.6	1979.7	1977.5
52	0.7	4.1×10^{-4}	1976.3	1977.5	1975.0
54	1.9	12.6×10^{-4}	1973.7	1975.0	1972.4
56	1.8	10.5×10^{-4}	1971.3	1972.4	1970.2
60	1.9	10.6×10^{-4}	1966.8	1967.9	1965.6
64	2.2	12.7×10^{-4}	1962.6	1963.5	1961.6
68	2.2	12.2×10^{-4}	1958.8	1959.7	1957.9
80	1.6	8.4×10^{-4}	1946.0	1947.3	1944.8
90	2.3	11.9×10^{-4}	1931.8	1933.8	1929.9
Avg.	1.7	13.5×10^{-4}			

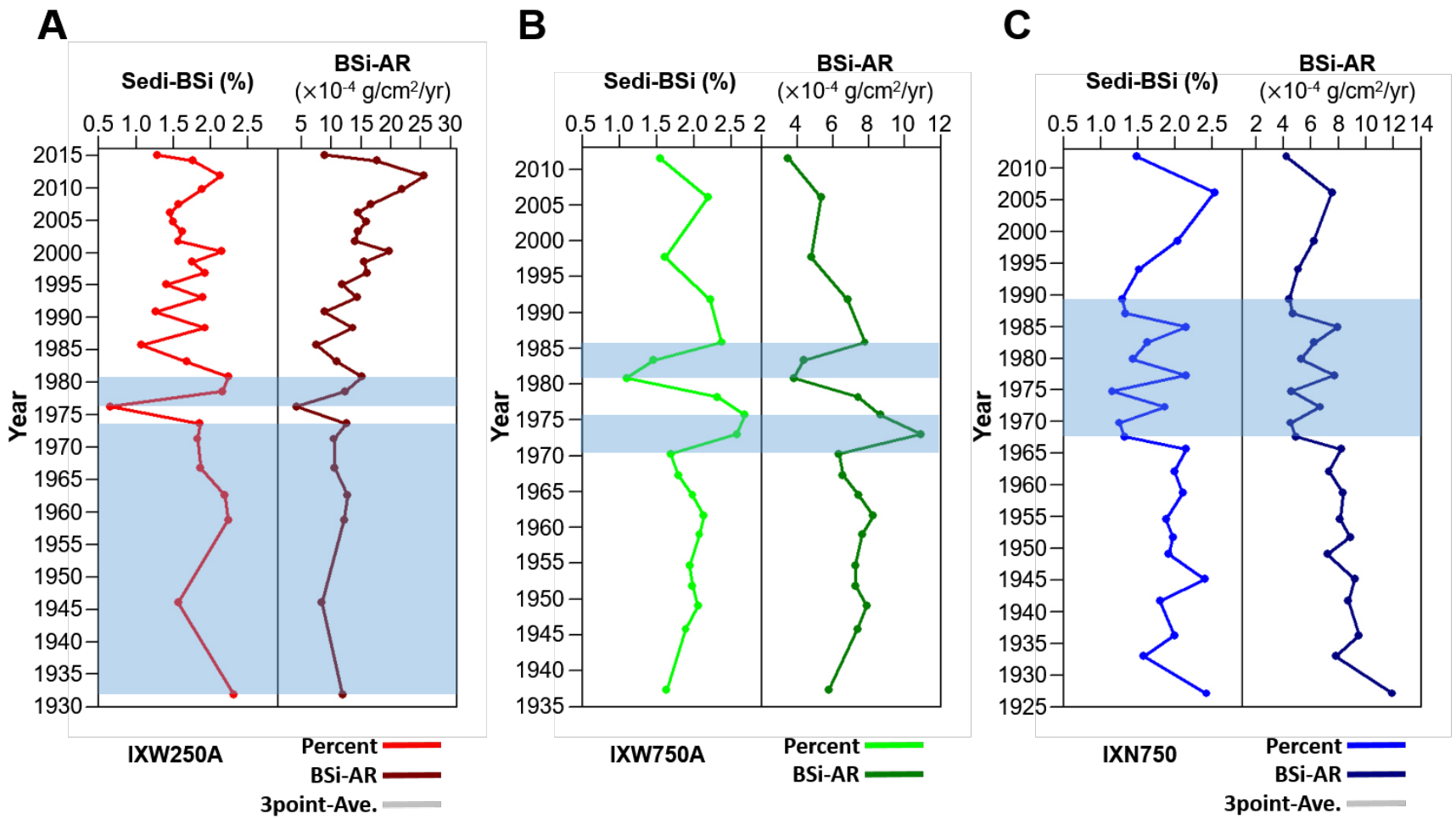

Fig 4. Profiles of Sedi-BSi with age of each cores collected in the SGOM (Left: Sedi-BSi contents, Right: BSi-AR). A: Profile of core from site IXW250A, B: Profile of core from site IXW750A, C: Profile of core from site IXN750

3.4 Discussion

3.4.1 Potential mechanisms for Sedi-BSi variation in the SGOM

The Sedi-BSi is controlled by variations in surface water primary productivity (Nelson et al., 1995; Tréguer et al., 1995). Environmental changes influence surface water productivity and deposition of byproducts to the seafloor (Nelson et al., 1995; Tréguer et al., 1995). A comprehensive understanding of anthropogenic influences and changed natural environment inputs is important and necessary to restrict mechanisms for variation of Sedi-BSi

Primary productivity in the SGOM, including this research area, is known to be highly related to variation in the discharge of the river systems, which supply fresh water to these areas (Gómez, 2002; Kemp et al., 2016; Martínez-López and Zavala-Hidalgo, 2009; Ruiz-Fernández et al., 2012; Salmeron-Garcia et al., 2011; Zavala-Hidalgo et al., 2003; Zavala-Hidalgo et al., 2006). Discharge of river systems in this region are controlled by human activity (e.g. dam constructions and operations of dam and artificial structure) and natural variation, including seasonal or inter-annual climate event (e.g. El Niño, La Niña, hurricane, and tropical storm) (Fabian Rivera-Trejo et al., 2010; Graia et al., 2013; Hudson et al., 2005; Kemp et al., 2016; Marengo, Athie & Calahorra, 2006; Lázaro-Vázquez et al., 2018; Muñoz-Salinas and Castillo, 2015; Ruiz-Fernández et al., 2012; Signoret et al., 2006; Sonnenfeld, 1992). The Grijalva-Usumacinta river system and the Papaloapan river system are affected by human activities because the Mexican government has constructed dams on these river systems (Fabian Rivera-Trejo et al., 2010; Marengo, Athie & Calahorra, 2006; Sonnenfeld, 1992).

According to results of this study, the level of Sedi-BSi was altered responding to dam constructions on the Grijalva river system and Papaloapan river system. Specifically, variation in

the Sedi-BSi when dams were constructed correlated with the relative location between coring sites and these rivers' mouths.

Sedi-BSi decreased when dams were constructed to the west of coring sites. And Sedi-BSi also decreased corresponding to dam constructions when the area is close to the river mouth and located on continental shelf area. Sedi-BSi tended to increase when dams were constructed at to the east of coring sites. The Grijalva-Usumacinta river system's mouth is located on the east side of site IXW750A. The river mouth of the Grijalva-Usumacinta river system is located on west side of IXN750. And site IXW250A is located on the continental shelf area and relatively close to river mouth of the Grijalva-Usumacinta river system. The Papaloapan River mouth is on the west side of site IXW750A.

Sedi-BSi also changed relative to the IXTOC-I oil spill in one sediment core from site IXW250A, which is the closest coring site to the IXTOC-1 wellhead and indicates a distinctive peak of Sedi-BSi in the sedimentary interval that corresponds to the IXTOC-I event.

Dam constructions

Discharge rates of the Grijalva-Usumacinta river system and Papaloapan river system have been controlled and influenced predominantly by natural and seasonal impacts (Kemp et al., 2016; Lázaro-Vázquez et al., 2018; Muñoz-Salinas and Castillo, 2015; Signoret et al., 2006). These two river systems play a role in primary nutrient sources in the Bay of Campeche area (Gracia et al., 2013; Jernelöv and Lindén, 1981; Kemp et al., 2016; Martínez-López and Zavala-Hidalgo, 2009; Salmerón-García et al., 2011). Their discharge has been influenced by natural or seasonal impacts, as well as primary productivity of the SGOM (Gómez, 2002; Martínez-López

and Zavala-Hidalgo, 200; Morey et al, 2005; Signoret et al., 2006; Zavala-Hidalgo et al., 2003; Zavala-Hidalgo et al., 2006; Zavala-Hidalgo et al., 2014).

After the 1940's, four major dams were constructed on the Grijalva river system (Malpaso dam, 1959 to 1964; Angostura dam, 1969 to 1974; Chicoasén dam, 1974 to 1980; Peñitas dam, 1979 to 1986). Two major dams had been constructed on the Papaloapan river system: Miguel Alemán dam, 1949 to 1954, and Cerro de Oro dam, 1973 to 1989. The main purpose of these series of the dam constructions was controlling the discharge rates of these rivers to minimize flood damages and generate electricity (Fabian Rivera-Trejo et al., 2010; Marengo, Athie & Calahorra, 2006; Sonnenfeld, 1992). Thus, the primary productivity of the SGOM has been influenced by the change in the input of material from the river water caused by dam constructions (Muñoz-Salinas and Castillo, 2015).

Nutrients from these two river systems move predominately from east to west (up-coast) at shelf area of the Bay of Campeche by the along-coast current during December to September (Martínez-López and Zavala-Hidalgo, 2009; Morey et al, 2005; Salmeron-Garcia et al., 2011; Zavala-Hidalgo et al., 2003; Zavala-Hidalgo et al., 2006; Zavala-Hidalgo et al., 2014). These shelf area nutrients are transported and redistributed to the deep ocean, outer shelf, including site IXW750A and site IXN750 by the Cross-shelf transport, which is formed seasonally during Autumn and Winter (September to February) (Dubranna et al., 2011; Martínez-López and Zavala-Hidalgo, 2009; Morey et al, 2005; Salmeron-Garcia et al., 2011; Zavala-Hidalgo et al., 2003; Zavala-Hidalgo et al., 2006; Zavala-Hidalgo et al., 2014). The highest chlorophyll-a (Chl-a) concentrations, including site IXN750, has been observed during September with the formation of the Cross-shelf transport and high discharge of the Usumacinta River (Dubranna et al., 2011; Hudson et al., 2005; Martínez-López and Zavala-Hidalgo, 2009; Morey et al, 2005; Muñoz-

Salinas and Castillo, 2015; Salmeron-Garcia et al., 2011; Signoret et al., 2006; Zavala-Hidalgo et al., 2003; Zavala-Hidalgo et al., 2006; Zavala-Hidalgo et al., 2014). Relatively high concentrations of Chl-a are maintained until December (Dubranna et al., 2011; Hudson et al., 2005; Martínez-López and Zavala-Hidalgo, 2009; Morey et al, 2005; Muñoz-Salinas and Castillo, 2015; Salmeron-Garcia et al., 2011; Signoret et al., 2006; Zavala-Hidalgo et al., 2003; Zavala-Hidalgo et al., 2006; Zavala-Hidalgo et al., 2014). In the case of the area including site IXW750A, higher concentrations of Chl-a has been observed in combination with net movement of water mass from west to east on shelf area during July to January, with a peak in October annually with formation of the Cross-shelf transport (Dubranna et al., 2011; Hudson et al., 2005; Muñoz-Salinas and Castillo, 2015; Martínez-López and Zavala-Hidalgo, 2009; Morey et al, 2005; Salmeron-Garcia et al., 2011; Signoret et al., 2006; Zavala-Hidalgo et al., 2003; Zavala-Hidalgo et al., 2006; Zavala-Hidalgo et al., 2014).

After the dam constructions on these two river systems, input of fresh water to the SGOM transitioned from seasonal and highly variable to stable and under control (Fabian Rivera-Trejo et al., 2010; Lázaro-Vázquez et al., 2018; Marengo, Athie & Calahorra, 2006; Papaloapan Ref). Dam constructions on the Grijalva river system caused the amount of freshwater input to shelf areas to fluctuate less (Fabian Rivera-Trejo et al., 2010; Lázaro-Vázquez et al., 2018; Marengo, Athie & Calahorra, 2006). However, the Grijalva River and Usumacinta River meet before draining into open water (Day et al., 2013). The Usumacinta river system is dam free and its discharge still fluctuates seasonally (Fabian Rivera-Trejo et al., 2010; Gracia et al., 2013; Hudson et al., 2005; Lázaro-Vázquez et al., 2018; Marengo, Athie & Calahorra, 2006; Muñoz-Salinas and Castillo, 2015). Thus, the amount of freshwater input from the Grijalva-Usumacinta river system decreases during high discharge and the Cross-shelf transport current formation

period (September to October) (Fabian Rivera-Trejo et al., 2010; Lázaro-Vázquez et al., 2018; Marengo, Athie & Calahorra, 2006; Muñoz-Salinas and Castillo, 2015). Coincidently, it is estimated that dam construction's influence over the input of nutrients to site IXN750 by the cross-shelf transport was decreased. Also, primary production was decreased compared to before dam constructions. This is corroborated by the lower Sedi-BSi of 20-38 mm (1968 ~ 1989) at site IXN750, consistent with the period of continuing construction (1969 ~ 1986) on the Grijlava river system. As the amount of discharge increased during low discharge periods, more nutrients could be transported to site IXW750A compared to before dam constructions by the along-coast current from east to west and the cross-shelf transport (Fabian Rivera-Trejo et al., 2010; Lázaro-Vázquez et al., 2018; Muñoz-Salinas and Castillo, 2015). Consequently, additional nutrients could be available at site IXW750A for primary production during these periods compared to before dam constructions. This is observed through the increases in the Sedi-BSi at 24 mm to 20 mm (1981 ~ 1986) and 32 mm to 28 mm (1970 ~ 1976) of cores from site IXW750A. These Layers are consistent with construction periods of the Peñitas dam (1979 ~ 1986) and the Angostura dam (1969 ~ 1974) on the Grijalva river system respectively.

In the case of dam constructions on the Papaloapan river system, these caused the amount of discharge to decrease during the period of high discharge and the period of the Cross-shelf transport formation (September to October). The amount of discharge was estimated to be increased during the period of low discharge. Thus, the primary productivity in the area including site IXW750A decreased compared to before dam constructions, in that nutrient availability was decreased during the phytoplankton blooming period. This is observed through a decrease in Sedi-BSi at 28 mm to 24 mm (1976 ~ 1981) of the core site IXW750, which is

matched with the Cerro de Oro dam construction period (1973 ~ 1989) on the Papaloapan river system.

IXTOX-I oil spill

A peak of Sedi-BSi contents in the core profile was observed at a core from site IXW250A after the IXTOC-I oil spill (50 mm to 48 mm). Chronology data of this peak (1980) indicated this peak correlated to right after the IXTOC-I oil spill. However, distinctively altered values were not observed at cores from site IXW750A and site IXN750 after the IXTOC-I oil spill. According to this study and variation of other environmental proxies, this peak is interpreted as consequence of the IXTOC-I oil spill in 1979.

The MOSSFA event was estimated to cause these increases in the Sedi-BSi contents. Environmental conditions surrounding site IXW250A were more likely suitable for the occurrence of the MOSSFA event, with the three main factors of MOS formation being river influences, marine biota, oil and dispersant (Daly et al., 2016; Passow et al., 2012; Passow and Ziervogel, 2016).

This is most likely due to site IXW250A being closer to the river mouth, the continental shelf area, and the blowout site than site IXW750A and site IXN750. The oil concentrations of an area adjacent to site IXW250A were consistently higher than the two other sites (Boehm and Flest, 1982; Farrington, 1980). Currents and primary production of an area adjacent to site IXW250A have been more influenced by the wind-driven, the along-coast current and upwelling by Ekman transport (Gómez, 2002; Martínez-López and Zavala-Hidalgo, 2009; Morey et al, 2005; Salmeron-Garcia et al., 2011; Zavala-Hidalgo et al., 2003; Zavala-Hidalgo et al., 2006; Zavala-Hidalgo et al., 2014). The nutrient input from the Grijalva-Usumacinta river systems is consistently higher level annually (Carranza-Edwards et al., 1993; Signoret et al., 2006). The

primary productivity is generally higher than the two other sites (Martínez-López and Zavala-Hidalgo, 2009; Morey et al, 2005; Salmerón-García et al., 2011; Zavala-Hidalgo et al., 2006). Thus, it is expected that more Exopolymeric Substance (EPS), which is a sticky substance secreted by surface water dwelling organisms (primary producers and consumers) that provide a matrix for the aggregation of particles for forming marine snow (Passow et al., 2012; Passow et al., 2016; Passow and Ziervogel, 2016), was supplied to the water column of site IXW250A with higher phytoplankton and toxicity of spilled oil. The clay mineral input to site IXW250A was higher than the two other sites (Carranza-Edwards et al., 1993; Signoret et al., 2006). As the outer shelf area, including site IXW750A and site IXN750, is isolated by the current from the shelf area, transport of the suspended sediment input is restricted (Carranza-Edwards et al., 1993; Dubranna et al., 2011; Hudson et al., 2005; Muñoz-Salinas and Castillo, 2015; Martínez-López and Zavala-Hidalgo, 2009; Morey et al, 2005; Salmeron-Garcia et al., 2011; Signoret et al., 2006; Zavala-Hidalgo et al., 2003; Zavala-Hidalgo et al., 2006; Zavala-Hidalgo et al., 2014). It is reported that suspended sediment from the river in this area is made up primarily of silt and clay particles (Carranza-Edwards et al., 1993; Signoret et al., 2006). Thus, the MOSSFA event is expected to occur in the area adjacent to site IXW250A and this is the main mechanism for an increase in the Sedi-BSi contents correlated to the IXTOC-I oil spill.

Higher oil concentrations were found in an area adjacent to site IXW750A after the first three months of the IXTOC-I blowout (June, July, and August, 1979) (Boehm and Flest, 1982; Farrington, 1980). However, this period was not matched with the period of formation of the Cross-shelf transport and seasonal phytoplankton blooming season. Plus, the dam “Cerro de Oro” (1979 to 1983) constructed on the Papaloapan river system caused input of the suspended sediment and nutrients to the site IXW750A to decrease during this period. Oil concentrations at

area adjacent to site IXN750 was higher after seasonal currents (the along-coast current) shifts (October to December) (Boehm and Flest, 1982; Farrington, 1980). This period coincided with phytoplankton blooming seasons in this area. However, serial dam constructions (1959 ~ 1986) resulted in decreases of outflowing nutrients and clay mineral. Thus, the environmental conditions surrounding site IXW750A and site IXN750 were not suitable for enhancement of MOSSFA. This may explain the distinctive variations of the Sedi-BSi contents could not be observed at these two sites.

3.4.2 Comparison with DWH Oil Spill

The Sedi-BSi of cores from the NGOM consistently increased after the DWH blowout. However, in the case of the IXTOC-I oil spill in the SGOM, only site IXW250A showed increased value after the oil spill.

The magnitude of variation of Sedi-BSi of cores used in this study caused by natural or anthropogenic hydrological changes, was around 68.7% (Sedi-BSi contents) and 69.8% (BSi-AR). However, the peak from profiles of site IXW250A was 245.1% (Sedi-BSi contents) and 269.0% (BSi-AR) increases. The fact that the magnitude of Sedi-BSi increases in sediment cores from the NGOM after the DWH blowout was up to 278.0% (Sedi-BSi contents) and 322.4% (BSi-AR) supports that this peak of the IXW250A was derived by IXTOC-I oil spill.

These variations of Sedi-BSi can be described through correlations between variation of river discharge in the study area and Sedi-BSi. Diatom blooms and increased clay-sized mineral input were observed after the DWH blowout at the NGOM, including coring sites in this research (Brooks et al., 2015; Hu at al., 2011; Romero et al., 2015; Yan et al., 2016). However, in the case of the IXTOC-I oil spill, the river input was not changed in response to the oil spill. Thus,

primary productivity and clay-sized mineral input had been controlled by seasonal variation of environments during the oil spill period in the Bay of Campeche area. Enhanced phytoplankton blooms were not expected to occur during the IXTOC-I oil spill. Water column primary productivity, clay and silt particle concentrations in the Bay of Campeche, adjacent to site IXW250A, sustained higher levels throughout the years because of the proximity to the river mouth, currents, and upwelling (Carranza-Edwards et al., 1993; Signoret et al., 2006). But the clay mineral transport to outer shelf including site IXW750A and site IXN750 were limited because these sites were further distance from the river mouth and separated by currents (Carranza-Edwards et al., 1993; Gómez, 2002; Martínez-López and Zavala-Hidalgo, 2009; Morey et al, 2005; Salmeron-Garcia et al., 2011; Signoret et al., 2006; Zavala-Hidalgo et al., 2003; Zavala-Hidalgo et al., 2006; Zavala-Hidalgo et al., 2014). Consequently, when comparing these two oil spills, increases of the Sedi-BSi are the consequence of the oil spill and MOSSFA event. This could have happened coincidently with phytoplankton blooms and enough clay-sized mineral input as well as adding oil and dispersants during phytoplankton blooming periods.

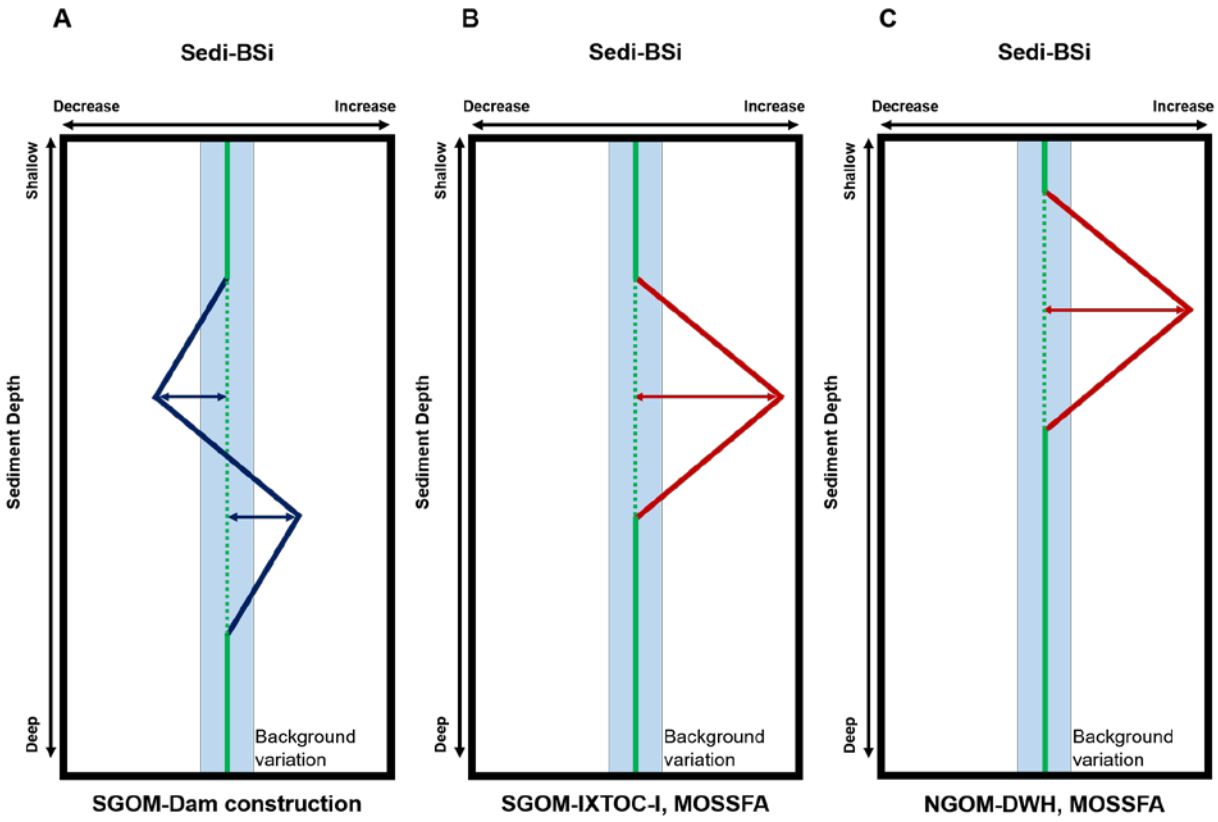

Fig 5. Summary for variation in Sedi-BSi after each impacts which are dam construction, Oil spill-IXTOC-I, DWH with MOSSFA event in the SGOM and the NGOM. A: Variation in Sedi-BSi caused by Dam construction. B: Variation in Sedi-BSi caused by IXTOC-I and ensuing MOSSFA event. C: Variation in Sedi-BSi caused by DWH and ensuing MOSSFA event.

3.5 Conclusions

Anthropogenic (e.g. dam constructions, IXTOC-I oil spill) environmental changes in the SGOM were tracked by studying variation in Sedi-BSi. Effects of the IXTOC-I oil spill were observed by comparing the Sedi-BSi profiles of cores from different locations influenced by oil spills with different surrounding environmental factors. By comparing profiles of Sedi-BSi contents of cores from the NGOM (DWH spill) and the SGOM (IXTOC-I), variations in massive oil spills were studied. Influences of the dam construction on the surface water diatom productivity were also studied. For this, the profiles of the Sedi-BSi of cores from the SGOM

were compared related to history of dam construction on the Grijalva river system and the Papaloapan river system.

There was a relatively large increase in the Sedi-BSi contents found in one core (site IXW250A) from the SGOM that correlated to the IXTOC-I oil spill, with the IXW750A and IXN750 cores lacking correlation. These increased values were distinctively larger increments compared to other variations of Sedi-BSi contents estimated to be caused by other seasonal variation and/or dam constructions. This is because of different environmental factors surrounding core's sites. The environmental factors surrounding the site IXW250A, which has a higher availability of nutrient and clay mineral from the river, higher diatom productivity, and higher oil concentration found in adjacent areas, were more favorable for the occurrence of MOSSFA event. These increased values' chronology data indicated right after the IXTOC-I oil spill. Thus, the more diatom frustules could be preserved and transported to seafloor. At the NGOM, the Sedi-BSi increased for all research areas after the DWH oil spill. These areas were exposed to suitable environmental condition that allowed for the MOSSFA events occur. This supports that the increases of Sedi-BSi coincided with the MOSSFA event. These increased values after the DWH oil spill and the IXTOC-I oil spill were recovered to the values before these oil spill after 3 to 6 years.

According to this research, dam constructions on the Grijalva river system and the Papaloapan river system resulted in variation of the primary productivity in the Bay of Campeche area. These variation of the primary productivity caused by dam constructions were observed in the profiles of Sedi-BSi from cores collected in the SGOM. Dam constructions induced decreasing Sedi-BSi in areas located to the east side of the river mouth and increasing in areas located to the west side of the river mouth. When the dam was constructed on the Grijalva

river system, Sedi-BSi ncreased at the site IXW750A and decreased at the site IXN750. Dam constructions on the Papaloapan river system caused Sedi-BSi to decrease at the site IXW750A.

Relative effects of dam constructions and IXTOC-I oil spill were documented in this research. These effects were highly influenced by surrounding environmental condition and seasonal natural variations. Freshwater discharge management during oil spill response is not only important to limit coastline oil contamination, but also affects the formation and intensity of MOSSFA and its consequence to the benthic community. Considering these points for creating remediation plans for future oil spills and anthropogenic hydrological changes could reduce the detrimental impacts.

3.6 References

Appleby, P.G. and Oldfieldz, F., 1983. The assessment of 210Pb data from sites with varying sediment accumulation rates. *Hydrobiologia*, *103*(1), pp.29-35.

Binford, M.W., 1990. Calculation and uncertainty analysis of 210 Pb dates for PIRLA project lake sediment cores. *Journal of Paleolimnology*, *3*(3), pp.253-267.

Boehm, P.D. and Fiest, D.L., 1982. Subsurface distributions of petroleum from an offshore well blowout. The Ixtoc I blowout, Bay of Campeche. *Environmental Science & Technology*, *16*(2), pp.67-74.

Brooks, G.R., Larson, R.A., Schwing, P.T., Romero, I., Moore, C., Reichart, G.J., Jilbert, T., Chanton, J.P., Hastings, D.W., Overholt, W.A. and Marks, K.P., 2015. Sedimentation pulse in the NE Gulf of Mexico following the 2010 DWH blowout. *PLoS One*, *10*(7), p.e0132341.

Carranza-Edwards, A., Rosales-Hoz, L. and Monreal-Gómez, A., 1993. Suspended sediments in the southeastern Gulf of Mexico. *Marine Geology*, *112*(1-4), pp.257-269.

Daly, K.L., Passow, U., Chanton, J. and Hollander, D., 2016. Assessing the impacts of oil-associated marine snow formation and sedimentation during and after the Deepwater Horizon oil spill. *Anthropocene*, *13*, pp.18-33.

Day, J.W., Mitsch, W.J. and Yanez-Arancibia, A., 2013. Using ecotechnology to address water and habitat loss quality in estuarine systems, Gulf of Mexico: a synthesis. *WIT Transactions on State-of-the-art in Science and Engineering*, *64*.

DeMaster, D.J., 1981. The supply and accumulation of silica in the marine environment. *Geochimica et Cosmochimica acta*, *45*(10), pp.1715-1732.

Dubranna, J., Pérez-Brunius, P., López, M. and Candela, J., 2011. Circulation over the continental shelf of the western and southwestern Gulf of Mexico. *Journal of Geophysical Research: Oceans*, *116*(C8).

Farrington, 1980. NOAA Ship RESEARCHER/Contract Vessel PIERCE Cruise to IXTOC-I Oil Spill: Overview and Integrative Data Assessment and Interpretation. National Oceanic and Atmospheric Administration

Gómez, R.A., 2002. Primary production in the southern Gulf of Mexico estimated from solar-stimulated natural fluorecence. *Hidrobiológica*, *12*(1), pp.21-28.

Gracia, A., Enciso Sánchez, G., Alexander Valdés, H.M. Composición y volúmen de contaminantes de las descargas costeras al Golfo de México. In: Botello, A.V., Rendón von Osten, J., Benítez, J., Gold-Bouchet, G. (eds) Golfo de México. Contaminación e impacto ambiental: diagnóstico y tendencias. uac, unam-icmyl, cinvestav-Unidad Mérida, 2013.

Hernández-Becerril, D.U., García-Reséndiz, J.A., Monreal-Gomez, M.A., Signoret-Poillon, M. and Aldeco-Ramirez, J., 2008. Nanoplankton fraction in the phytoplankton structure in the southern Gulf of Mexico (April 2000). *Ciencias Marinas*, *34*(1), pp.77-90.

Hu, C., Weisberg, R.H., Liu, Y., Zheng, L., Daly, K.L., English, D.C., Zhao, J. and Vargo, G.A., 2011. Did the northeastern Gulf of Mexico become greener after the Deepwater Horizon oil spill?. *Geophysical Research Letters*, *38*(9).

Hudson, P.F., Hendrickson, D.A., BENKE, A.C., VARELA-ROMERO, A.L.E.J.A.N.D.R.O., RODILES-HERNÁNDEZ, R.O.C.I.O. and Minckley, W.L., 2005. Rivers of Mexico. In *Rivers of North America* (pp. 1030-1084).

Jernelöv, A. and Lindén, O., 1981. Ixtoc I: a case study of the world's largest oil spill. *Ambio*, pp.299-306.

Kemp, G., Day, J., Yáñez-Arancibia, A. and Peyronnin, N., 2016. Can continental shelf river plumes in the northern and southern Gulf of Mexico promote ecological resilience in a time of climate change?. *Water*, *8*(3), p.83.

Lázaro-Vázquez et al, A., Castillo, M.M., Jarquín-Sánchez, A., Carrillo, L. and Capps, K.A., 2018. Temporal changes in the hydrology and nutrient concentrations of a large tropical river: A nthropogenic influence in the L ower G rijalva R iver, M exico. *River Research and Applications*, *34*(7), pp.649-660.

Licea, S., Zamudio, M.E., Moreno-Ruiz, J.L. and Luna, R., 2011. A suggested local regions in the Southern Gulf of Mexico using a diatom database (1979-2002) and oceanic hidrographic features. *Journal of environmental biology*, *32*(4), p.443.

Marengo, H., Athie, L. and Calahorra, O., 2006. Extreme events in the Grijalva river hydroelectric system in the southeast of Mexico in 1999. *Dams and Reservoirs, Societies and Environment in the 21st Century*, pp.199-205.

Martínez-López, B. and Zavala-Hidalgo, J., 2009. Seasonal and interannual variability of cross-shelf transports of chlorophyll in the Gulf of Mexico. *Journal of Marine Systems*, *77*(1-2), pp.1-20.

Morey, S.L., Zavala-Hidalgo, J. and O'Brien, J.J., 2005. The seasonal variability of continental shelf circulation in the northern and western Gulf of Mexico from a high-resolution numerical model. *Circulation in the Gulf of Mexico: Observations and models*, pp.203-218.

Munoz-Salinas, Esperanza, and Miguel Castillo. "Streamflow and sediment load assessment from 1950 to 2006 in the Usumacinta and Grijalva Rivers (Southern Mexico) and the influence of ENSO." *Catena* 127 (2015): 270-278.

Nelson, D.M., Tréguer, P., Brzezinski, M.A., Leynaert, A. and Quéguiner, B., 1995. Production and dissolution of biogenic silica in the ocean: revised global estimates, comparison with regional data and relationship to biogenic sedimentation. *Global Biogeochemical Cycles*, *9*(3), pp.359-372.

Passow, U., Ziervogel, K., Asper, V. and Diercks, A., 2012. Marine snow formation in the aftermath of the Deepwater Horizon oil spill in the Gulf of Mexico. *Environmental Research Letters*, *7*(3), p.035301.

Passow, U. and Ziervogel, K., 2016. Marine snow sedimented oil released during the Deepwater Horizon spill. *Oceanography*, *29*(3), pp.118-125.

Rivera-Trejo, F., Soto-Cortés, G. and Méndez-Antonio, B., 2010. The 2007 flood in Tabasco, Mexico: An integral analysis of a devastating phenomenon. *International Journal of River Basin Management*, *8*(3-4), pp.255-267.

Romero, I.C., Schwing, P.T., Brooks, G.R., Larson, R.A., Hastings, D.W., Ellis, G., Goddard, E.A. and Hollander, D.J., 2015. Hydrocarbons in deep-sea sediments following the 2010 Deepwater Horizon blowout in the northeast Gulf of Mexico. *PLoS One*, *10*(5), p.e0128371.

Ruiz-Fernandez, A.C., Sanchez-Cabeza, J.A., Alonso-Hernandez, C., Martínez-Herrera, V., Perez-Bernal, L.H., Preda, M., Hillaire-Marcel, C., Gastaud, J. and Quejido-Cabezas, A.J., 2012. Effects of land use change and sediment mobilization on coastal contamination (Coatzacoalcos River, Mexico). *Continental Shelf Research*, *37*, pp.57-65.

Salmerón-García, O., Zavala-Hidalgo, J., Mateos-Jasso, A. and Romero-Centeno, R., 2011. Regionalization of the Gulf of Mexico from space-time chlorophyll-a concentration variability. *Ocean Dynamics*, *61*(4), pp.439-448.

Schwing, P.T., Romero, I.C., Larson, R.A., O'Malley, B.J., Fridrik, E.E., Goddard, E.A., Brooks, G.R., Hastings, D.W., Rosenheim, B.E., Hollander, D.J. and Grant, G., 2016. Sediment core extrusion method at millimeter resolution using a calibrated, threaded-rod. *Journal of visualized experiments: JoVE*, (114).

Schwing, P.T., Brooks, G.R., Larson, R.A., Holmes, C.W., O'Malley, B.J. and Hollander, D.J., 2017. Constraining the Spatial Extent of Marine Oil Snow Sedimentation and Flocculent Accumulation Following the Deepwater Horizon Event Using an Excess 210Pb Flux Approach. *Environmental Science & Technology*, *51*(11), pp.5962-5968.

Signoret, M., Monreal-Gómez, M.A., Aldeco, J. and Salas-de-León, D.A., 2006. Hydrography, oxygen saturation, suspended particulate matter, and chlorophyll-a fluorescence in an oceanic region under freshwater influence. *Estuarine, Coastal and Shelf Science*, *69*(1-2), pp.153-164.

Sonnenfeld, D.A., 1992. Mexico's" Green Revolution," 1940-1980: Towards an Environmental History. *Environmental History Review*, *16*(4), pp.29-52.

Treguer, P., Nelson, D.M., Van Bennekom, A.J., DeMaster, D.J., Leynaert, A. and Quéguiner, B., 1995. The silica balance in the world ocean: a reestimate. *Science*, *268*(5209), pp.375-379.

Yan, B., Passow, U., Chanton, J.P., Nöthig, E.M., Asper, V., Sweet, J., Pitiranggon, M., Diercks, A. and Pak, D., 2016. Sustained deposition of contaminants from the Deepwater Horizon spill. *Proceedings of the National Academy of Sciences*, *113*(24), pp.E3332-E3340.

Zavala-Hidalgo, J., Morey, S.L. and O'Brien, J.J., 2003. Seasonal circulation on the western shelf of the Gulf of Mexico using a high-resolution numerical model. *Journal of Geophysical Research: Oceans*, *108*(C12).

Zavala-Hidalgo, J., Gallegos-García, A., Martínez-López, B., Morey, S.L. and O'Brien, J.J., 2006. Seasonal upwelling on the western and southern shelves of the Gulf of Mexico. *Ocean dynamics*, *56*(3-4), pp.333-338.

Zavala-Hidalgo, J., Romero-Centeno, R., Mateos-Jasso, A., Morey, S.L. and Martinez-Lopez, B., 2014. The response of the Gulf of Mexico to wind and heat flux forcing: What has been learned in recent years?. *Atmósfera*, *27*(3), pp.317-334.